ISSN 2182-1976

Recreational Mathematics Magazine

Number 5
March, 2016

DE GRUYTER OPEN
Ludus
CIUHCT

Edition
Associação Ludus, Museu Nacional de História Natural e da Ciência,
Rua da Escola Politécnica 56 1250-102 Lisboa, Portugal

email: rmm@ludus-opuscula.org
URL: http://rmm.ludus-opuscula.org

Managing Editor
Carlos Pereira dos Santos, cmfsantos@fc.ul.pt
Center for Linear Structures and Combinatorics, University of Lisbon

Editorial Board
Aviezri S. Fraenkel, Aviezri.Fraenkel@weizmann.ac.il, Weizmann Institute
Carlos Pereira dos Santos
Colin Wright, juggler@solipsys.co.uk, Liverpool Mathematical Society
David Singmaster, zingmast@gmail.com, London South Bank University
David Wolfe, davidgameswolfe@gmail.com, Gustavus Adolphus College
Edward Pegg, ed@mathpuzzle.com, Wolfram Research
João Pedro Neto, jpn@di.fc.ul.pt, University of Lisbon
Jorge Nuno Silva, jnsilva@cal.berkeley.edu, University of Lisbon
Keith Devlin, kdevlin@stanford.edu, Stanford University
Richard Nowakowski, rjn@mathstat.dal.ca, Dalhousie University
Robin Wilson, r.j.wilson@open.ac.uk, Open University
Thane Plambeck, tplambeck@gmail.com, Counterwave, inc

Informations
The *Recreational Mathematics Magazine* is electronic and semiannual.
The issues are published in the exact moments of the equinox.
The magazine has the following sections (not mandatory in all issues):

Articles
Games and Puzzles
Problems
MathMagic
Mathematics and Arts
Math and Fun with Algorithms
Reviews
News

ISSN 2182-1976

Contents

Page

Articles: ***Jörg Pretz***
The triangular binary clock **5**

Articles: ***Chia-Yu Lin***
Digital root patterns of three-dimensional space **9**

Mathematics and Arts: ***Alda Carvalho, Carlos Pereira dos Santos, Jorge Nuno Silva***
Allgorie de la Gomtrie: A mathematical interpretation **33**

Games and Puzzles: ***Robert Bates Graber, Stephen Pollard, Ronald C. Read***
Star tangrams **47**

Games and Puzzles: ***Iain G. Johnston***
Endless love: On the termination of a playground number game **61**

Articles

The triangular binary clock

Jörg Pretz
III. Physikalisches Institut B, RWTH Aachen University
pretz@physik.rwth-aachen.de

Abstract: *A new idea for a binary clock is presented. It displays the time using a triangular array of* 15 *lamps each representing a certain amount of time. It is shown that such a geometric, triangular arrangement is only possible because our system of time divisions is based on a sexagesimal system in which the number of minutes in* 12 *hours equals the factorial of a natural number (*$720 = 6!$*). An interactive applet allows one to "play" with the clock.*

Key-words: binary, clock, time, sexagesimal system.

1 Introduction

There are many ways to display the time. For example the familiar analog display with a dial and clock hands or digital displays using numerals. In addition there are binary displays which are a bit more difficult to read. Here a lamp lit corresponds to a certain amount of time. The binary display presented in this article has the special feature that the lamps are arranged in form of a triangle.

In section 2 the clock is presented with the help of an interactive javascript applet. Section 3 illuminates the mathematical background and shows that the triangular display is only possible because our system of time divisions is based on a sexagesimal system rather than a decimal system (see also [1]).

2 The triangular clock

The following applet illustrates the idea. To read off the time you have to know that every lamp lit in the ...
... 1st line (top line) corresponds to 6h
... 2nd line corresponds to 2h
... 3rd line corresponds to 30 min
... 4th line corresponds to 6 min
... 5th line corresponds to 1 min
green is for AM and red for PM. You can play with the clock by using the buttons on the left. The allow one to advance or to move back the clock in steps

of one minute or one hour. To set the time back to the present time just push the top button. The two checkboxes allow for more help or to hide the time given in numerals in case you would like to train yourself. You will find out that all lamps on corresponds to 11:59 (green) or 23:59 (red). So this arrangement perfectly fits for a twelve hour display.

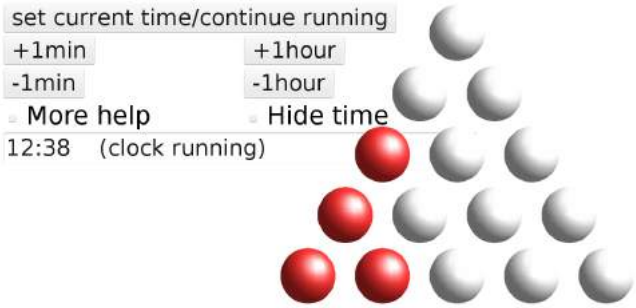

Applet online:

`http://web.physik.rwth-aachen.de/user/pretz/binary_clock/ludus/jpretz_binary_clock.htm`.

A few examples are shown below.

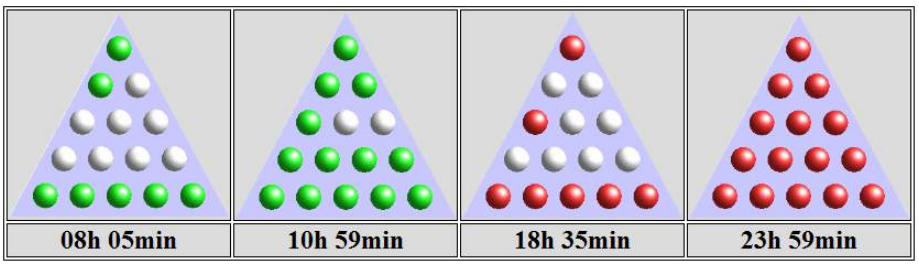

3 Mathematical background

We now come to the question why our system of time divisions allows such a triangular display? First note, that the amount of time, T_{n-1}, a lamp corresponds to in the $(n-1)$th row equals (m_n+1) times the amount, T_n, in the nth row where m_n is the number of lamps in the nth row. Thus,

$$T_{n-1} = (m_n + 1) \times T_n.$$

Here are two examples:

- The 3rd row has $m_3 = 3$ lamps representing 30 minutes each. Thus for the 2nd row one finds $(3 + 1) \times 30$ min $= 2$ h.
- The 5th row has $m_5 = 5$ lamps representing 1 minute each. Thus for the 4th row one finds $(5 + 1) \times 1$ min $= 6$ min.

The triangular display has the special feature that $m_n = n$, i.e. in the nth row there are also n lamps This is just the condition for a triangular display. But what does $m_n = n$ mean for the number of states which can be represented by the display? A row with n lamps allows one to display $n + 1$ states, from all lamps off to all lamps on. (Note that in the way the display is used here, not all of the 2^n possible states are used because if a lamp is on, also the lamps left to it are on in the same row.) For a triangular display with n lamps in the bottom row and the number of lamps decreasing by one in every following row the total number of states is thus,

$$(n + 1) \times ((n - 1) + 1) \times ((n - 2) + 1) \times \cdots \times (1 + 1) = (n + 1)!$$

i.e the number of states equals always a factorial of a natural number. Now, note that our system of time measurement is based on numbers which have many divisors, e.g. $12 = 3 \times 4$ and $60 = 1 \times 2 \times 5 \times 6$. For a 12 hour display with a precision of one minute the number of states one has to display is thus,

$$12 \times 60 \text{ minutes} = 1 \times 2 \times 3 \times 4 \times 5 \times 6 \text{ minutes} = 6! \text{ minutes.}$$

which perfectly fits in a triangular display with five rows! Thus the whole concept works because our system of time divisions is based on a sexagesimal system, dating back to the Babylonian [2, 3], rather than a decimal system, as proposed during the French Revolution [4, 5].

References

[1] Pretz, J. "A different way to read off the time – A new idea for a binary clock", *Journal of Recreational Mathematics*, Vol. 35(4), 327–330, arXiv:1006.1373v1 [math.HO], 2006.

[2] Neugebauer, O. *The Exact Sciences in Antiquity*, Barnes & Noble, New York, 1993.

[3] Wikipedia article. "Babylonia": `http://en.wikipedia.org/wiki/Babylonia`

[4] Richard A., Carrigan, Jr. "Decimal time", *American Scientist*, 305(78), 66, 1978.

[5] Wikipedia article. "Decimal time": `http://en.wikipedia.org/wiki/Decimal_time`

Articles

Digital root patterns of three-dimensional space

Chia-Yu Lin

Department of Hydraulic and Ocean Engineering, National Cheng Kung University, Tainan, Taiwan, 701

sharkgallium@gmail.com

Abstract: *In this study, we define vedic cube as the layout of each digital root in a three-dimensional multiplication table. In order to discover the geometric patterns in vedic cube, we adopt two methods to analyze the digital root in a three-dimensional space. The first method is floor method, which divides vedic cube into several X-Y planes according to different Z values (floors) to analyze the geometric characteristics on each floor. The second method is symmetric plane method, which decomposes vedic cube by its main and secondary symmetric planes.*

Key-words: Digital root, pattern, vedic square, vedic cube, symmetry.

1 Introduction

1.1 Digital root

Exploring regularity and pattern of numbers is the most fascinating experience in mathematical research. The discovery of digital root is one of those surprises. The digital root of a positive integer is the summation of each digit ranging from one to nine. For example, the digital root of 19 is the addition of 1 and 9, repeat the procedure until the final number ranges from one to nine. After calculation, the digital root of 19 is 1, in other words, addition mod 9. $D(N)$ is used to denote the digital root of a positive integer N. Digital root operation of 19 is listed as follows:

$$D(19) = D(1 + 9) = D(10) = D(1) = 1. \tag{1}$$

Recreational Mathematics Magazine, Number 5, pp. 9–31
DOI 10.1515/rmm–2016–0002

Vedic square is one of the most famous regularities discovered many centuries ago [10]. It is the layout of digital roots in a typical multiplication table shown in Figure 1, and the digital root of a specific point $D(X, Y)$ in vedic square can be calculated as

$$D(X, Y) = D(X \times Y) = D(D(X) \times D(Y)). \tag{2}$$

X and Y are any positive integers.

1.2 Vedic square and Islamic culture

Quran has profound influence in Islamic culture in perceiving values of life and expressions of art. Quran an prohibits the representation of the human figure in art; therefore Muslims perform their art in a sophisticated way using many geometric patterns to decorate Quran, architecture, pottery, and apparel. Muslims have incorporated vedic square into their mathematical system since 770 AD [10].

1	2	3	4	5	6	7	8	9
2	4	6	8	1	3	5	7	9
3	6	9	3	6	9	3	6	9
4	8	3	7	2	6	1	5	9
5	1	6	2	7	3	8	4	9
6	3	9	6	3	9	6	3	9
7	5	3	1	8	6	4	2	9
8	7	6	5	4	3	2	1	9
9	9	9	9	9	9	9	9	9

Figure 1: vedic square. It is the layout of digital roots in a 2-D multiplication table.

Some geometric characteristics in vedic square are including symmetry and complementation in digits, patterns in columns and rows. Figure 2 shows the patterns formed by each digital root, digital roots with summation of nine mirror each other along vertical line, including digit 1 versus 8, digit 2 versus 7, digit 3 versus 6, and digit 4 versus 5. vedic square can also be used to produce a new pattern, which is composed by a line of numbers from specific column or row in vedic square with a constant angle [7]. Furthermore, there are several literatures discussing geometric patterns of Islamic art [1, 11].

1.3 Element: from 2-D to 3-D space

Designer Cecil Balmond uses many informal concepts in designing architectural structure. In Serpentine Gallery Pavilion 2002 project designed by Toyo Ito, Cecil Balmond and Arup [6], Balmond used a simple element, a square, to develop specific half-to-a-one-third algorithm. The structure form was created by lining up the middle point of one side to the one-third point of adjacent side.

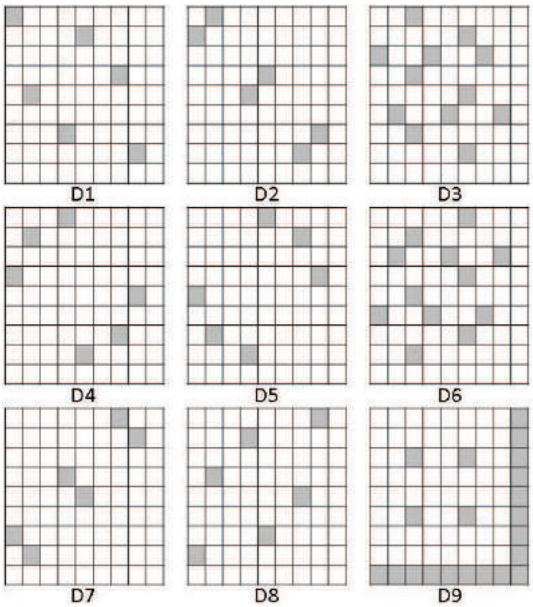

Figure 2: Patterns in vedic square. the patterns formed by each digital root, digital roots with summation of nine mirror each other along vertical line, including digit 1 versus 8, digit 2 versus 7, digit 3 versus 6, and digit 4 versus 5.

Repeat the procedure at four sides of the square and stretch the sides out of the original square, then a smaller square compared to the original one can be generated. Follow this rule, the result footprint is shown in Figure 3 [5]. Part of the footprint is selected as the constructing element of structures roof, the corners are cut, and the remaining part is folded as buildings supporting structure to form a box. Serpentine Gallery Pavilion 2002 is a great project developed from a simple element to a delicate masterpiece and provides the insight from 2-D to 3-D space. Balmond's works are often inspired by nature element, Islamic art, and numbers [3, 4].

So far, many studies have discussed about the digital root patterns in 2-D plane, and their characteristics in vedic square [2, 7, 9, 10]. However, there have been little discussions about digital root patterns in 3-D space. This study, inspired by the beauty of Islamic art [12] and Serpentine Gallery Pavilion 2002, aims to explore those undiscovered characteristics of digital roots, and the corresponding patterns in the 3-D space.

2 Vedic cube

Inspired by both Islamic art and Serpentine Gallery Pavilion 2002, this study assumes that there are more interesting digital root patterns in 3-D space yet to be uncovered. We create a three-dimensional multiplication table by adding Z-axis on the original one for further discussion, and also define a vedic cube

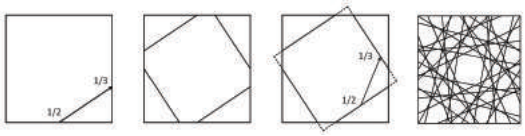

Figure 3: The half-to-a-one-third algorithm concept of Serpentine Gallery Pavilion 2002 (modified) [5].

as the digital root in a 3-D space created in this study. The side length of vedic cube is 9, and there are 729 points in it. Let $D(X, Y, Z)$ denote the digital root of a specific point (X, Y, Z) in vedic cube, which

$$D(X, Y, Z) = D(X \times Y \times Z) = D(D(X) \times D(Y) \times D(Z)). \tag{3}$$

As same as ´vedic square, X, Y and Z are any positive integers. An example of digital root operation is listed as follows: the value of point (2,3,5) in vedic cube is

$$D(2 \times 3 \times 5) = D(30) = D(3) = 3. \tag{4}$$

In this study, digital root M, digit M and $D(X, Y, Z) = M$ all denote digital root operational result.

In order to find out the digital root distribution in a 3-D space, Matlab software is used to calculate the digital root value of each number in vedic cube and plot specific digital roots. Figure 4 shows all points of digital root 1 scatter in vedic cube. Distribution of digital root 2, 3, 4 and 9 are shown in the Figure A-1 of appendices. Due to the difficulty in recognizing digital root patterns in 3-D space, we adopt two methods in this study to analyze and simplify the complexity of digital root patterns in vedic cube.

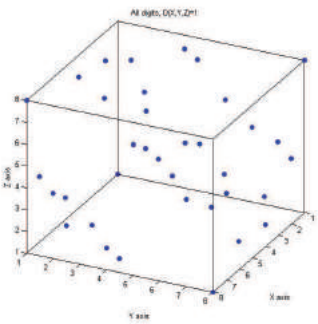

Figure 4: All points of digital root 1 in vedic cube. The pattern is too intricate to be recognized immediately.

3 Analysis methods, findings and explanations

3.1 Floor method: dividing vedic cube into floors

The first method is dividing vedic cube into several layers according to different Z value (X value or Y value is also feasible), which is similar to the floors of a building ranging from 1 to 9. Figure 5 illustrates all the digital roots on each floor. The order of the first floor ($F1$) to the ninth floor ($F9$) is defined from left to right, top to bottom. For example, the upper middle square in Figure 5 is the second floor with corresponding code defined as $F2$. The rest of the floors also possess exactly the same rule.

According to Figure 5, the digital root distribution can be categorized into three groups of digit. The group A of digit contains digit 1, 2, 4, 5, 7 and 8. Use digit 1 as example, each floor of $F1$, $F2$, $F4$, $F5$, $F7$, and $F8$ (Group α of floor) contains 6 points of digit 1. There are total 36 points of digit 1, six digits occupy 216 points in vedic cube within the defined 3-D space. The group B of digit contains digit 3 and 6. Use digit 3 as example, each floor of group α contains 12 points of digit 3. Each floor of $F3$ and $F6$ (Group β) contains 18 points of digit 3. There are total 108 points of digit 3. The group B of digit occupies 216 points in vedic cube within the defined 3-D space. The group C of digit is digit 9. Each floor of group α contains 21 points of digit 9. Each floor of group β contains 45 points of digit 9, and $F9$ (Group γ) contains 81 points. The group C of digit occupies 297 points in vedic cube. In total, the summation of all points of each digit is 729, which is equal to the total number of points in vedic cube.

3.2 Code definition of basic patterns and columns

In order to easily explain specific patterns, we create a code system to represent each basic pattern. The basic pattern has certain connection with digit's order of position occurring in vedic square. For example, pattern consisted of digit 1 on vedic square is defined as $D1F1$ with abbreviation as $D1$. Same rule is also used for digit 2 to digit 9 as $D2F1$, $D3F1$, $D4F1$, $D5F1$, $D6F1$, $D7F1$, $D8F1$ and $D9F1$, respectively. However, except the first floor ($F1$), the code of floor cannot be ignored in other floors. For example, the pattern of digit 1 on the second floor ($F2$) is defined as $D1F2$, pattern of digit 1 on third floor ($F3$) is defined as $D1F3$, etc. Furthermore, the column and row on vedic cube are also defined for further discussion. $C2F1$ denotes the second column ($C2$) of $F1$, which is consisting of nine numbers 2, 4, 6, 8, 1, 3, 5, 7, 9, as shown in Figure 5. Numbers in column and row are identical on vedic cube. Definition of Ch represents for both basic h^{th} column and row in vedic square, which is similar to the rule of basic patterns.

3.3 Characteristics of Digital root patterns in 3-D space

Several geometric characteristics of same digit can be found on the different floors. Take digit 1 for example, $D1F2$ (pattern on the second floor) is identical to $D5F1$, and $D1F7$ (pattern on the seventh floor) is identical to $D4F1$ (Figure 5). They mirror each other along the vertical line of projection onto the $X-Y$

1	2	3	4	5	6	7	8	9
2	4	6	8	1	3	5	7	9
3	6	9	3	6	9	3	6	9
4	8	3	7	2	6	1	5	9
5	1	6	2	7	3	8	4	9
6	3	9	6	3	9	6	3	9
7	5	3	1	8	6	4	2	9
8	7	6	5	4	3	2	1	9
9	9	9	9	9	9	9	9	9

F1

2	4	6	8	1	3	5	7	9
4	8	3	7	2	6	1	5	9
6	3	9	6	3	9	6	3	9
8	7	6	5	4	3	2	1	9
1	2	3	4	5	6	7	8	9
3	6	9	3	6	9	3	6	9
5	1	6	2	7	3	8	4	9
7	5	3	1	8	6	4	2	9
9	9	9	9	9	9	9	9	9

F2

3	6	9	3	6	9	3	6	9
6	3	9	6	3	9	6	3	9
9	9	9	9	9	9	9	9	9
3	6	9	3	6	9	3	6	9
6	3	9	6	3	9	6	3	9
9	9	9	9	9	9	9	9	9
3	6	9	3	6	9	3	6	9
6	3	9	6	3	9	6	3	9
9	9	9	9	9	9	9	9	9

F3

4	8	3	7	2	6	1	5	9
8	7	6	5	4	3	2	1	9
3	6	9	3	6	9	3	6	9
7	5	3	1	8	6	4	2	9
2	4	6	8	1	3	5	7	9
6	3	9	6	3	9	6	3	9
1	2	3	4	5	6	7	8	9
5	1	6	2	7	3	8	4	9
9	9	9	9	9	9	9	9	9

F4

5	1	6	2	7	3	8	4	9
1	2	3	4	5	6	7	8	9
6	3	9	6	3	9	6	3	9
2	4	6	8	1	3	5	7	9
7	5	3	1	8	6	4	2	9
3	6	9	3	6	9	3	6	9
8	7	6	5	4	3	2	1	9
4	8	3	7	2	6	1	5	9
9	9	9	9	9	9	9	9	9

F5

6	3	9	6	3	9	6	3	9
3	6	9	3	6	9	3	6	9
9	9	9	9	9	9	9	9	9
6	3	9	6	3	9	6	3	9
3	6	9	3	6	9	3	6	9
9	9	9	9	9	9	9	9	9
6	3	9	6	3	9	6	3	9
3	6	9	3	6	9	3	6	9
9	9	9	9	9	9	9	9	9

F6

7	5	3	1	8	6	4	2	9
5	1	6	2	7	3	8	4	9
3	6	9	3	6	9	3	6	9
1	2	3	4	5	6	7	8	9
8	7	6	5	4	3	2	1	9
6	3	9	6	3	9	6	3	9
4	8	3	7	2	6	1	5	9
2	4	6	8	1	3	5	7	9
9	9	9	9	9	9	9	9	9

F7

8	7	6	5	4	3	2	1	9
7	5	3	1	8	6	4	2	9
6	3	9	6	3	9	6	3	9
5	1	6	2	7	3	8	4	9
4	8	3	7	2	6	1	5	9
3	6	9	3	6	9	3	6	9
2	4	6	8	1	3	5	7	9
1	2	3	4	5	6	7	8	9
9	9	9	9	9	9	9	9	9

F8

9	9	9	9	9	9	9	9	9
9	9	9	9	9	9	9	9	9
9	9	9	9	9	9	9	9	9
9	9	9	9	9	9	9	9	9
9	9	9	9	9	9	9	9	9
9	9	9	9	9	9	9	9	9
9	9	9	9	9	9	9	9	9
9	9	9	9	9	9	9	9	9
9	9	9	9	9	9	9	9	9

F9

Figure 5: All digits from first floor ($F1$) to ninth floor ($F9$) in floor method analysis. The order of floors is from left to right, top to bottom.

plane (also for $Y - Z$ and $X - Z$ planes). Also, three pairs of patterns: $D1F1$ and $D1F8$, $D1F3$ and $D1F6$, $D1F4$ and $D1F5$, all possess exactly the same characteristics.

Since patterns of $F5$ to $F8$ can be mirrored along the vertical line onto $X - Y$ plane from $F1$ to $F4$, this part of the study focuses on analyzing $F1$ to $F4$. Patterns of digit 9 are easily to predict. For group α of floor, they occur on positions either when both X and Y are multiples of 3, or one of X and Y is 9. For group β, they occur when either X or Y is multiple of 3. For group γ ($F9$), all digits are 9 shown in Figure A-1(d) of appendices.

The study finds that patterns of specific digit on different floors in 3-D space follow special rule which can be indicated from vedic square (Figure 5 and Figure 6). Here is an example of digit 1, rule of digit 1 varying according to different floors is shown in Figure 6(a). Pattern in Figure 6(a) refers to which basic pattern (Figure 2) is identical to pattern of digit 1 on the Xth floor (FX).

In Figure 6(b), when X is 2, digit 1 occurs on the fifth position (Y=5). X refers to the second floor, while Y represents the order of patterns is 5 in Figure 6(a). It is concluded that $D1F2$ pattern is identical to $D5F1$ pattern. From Figure 6(b), the patterns of digit 1 on $F4$, $F5$, $F7$, and $F8$ can be indicated from $D7$, $D2$, $D4$, and $D8$ in vedic square.

The explanation of this can be traced back to digit 5 in vedic square, because only the product of 5 and 2 can result in digit 1, it perfectly explains why $D1F2$ is identical to $D5F1$. Other patterns on different floors also follow the same principle.

To check whether pattern of digit p on the qth floor ($DpFq$) is the same as pattern of digit r on the sth floor ($DrFs$), the following equation is used to identify:

$$\text{If } D(p \times s) = D(q \times r), \text{ then } DpFq = DrFs. \tag{5}$$

When s=1, Dr, which represents the corresponding basic pattern of $DpFq$, can be identified. Digits occupying Dr's position on Fq is digit p. In other words, digital root patterns of 3-D space can be identified from 2-D plane. vedic square is not just a part of vedic cube, it is the fundamental basis of digital root patterns in 3-D space.

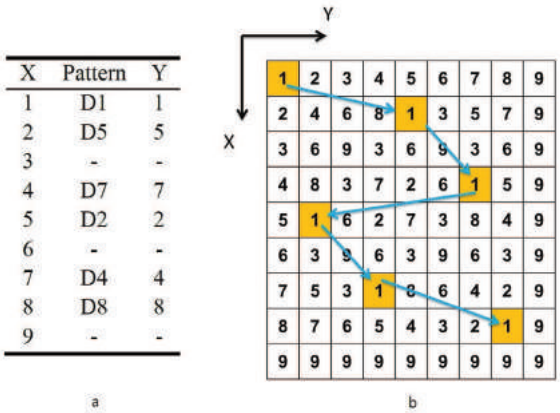

X	Pattern	Y
1	D1	1
2	D5	5
3	-	-
4	D7	7
5	D2	2
6	-	-
7	D4	4
8	D8	8
9	-	-

1	2	3	4	5	6	7	8	9
2	4	6	8	1	3	5	7	9
3	6	9	3	6	9	3	6	9
4	8	3	7	2	6	1	5	9
5	1	6	2	7	3	8	4	9
6	3	9	6	3	9	6	3	9
7	5	3	1	8	6	4	2	9
8	7	6	5	4	3	2	1	9
9	9	9	9	9	9	9	9	9

Figure 6: Rule of digit 1 is varying according to different floors. (a) Pattern refers to which basic pattern (Figure 2) is identical to pattern of digit 1 on the Xth floor (FX). (b) Patterns of specific digit on different floors in 3-D space follow special rule which can be indicated from vedic square. When X is 2, digit 1 occurs on the fifth position (Y=5). X refers to the second floor, while Y represents the order of patterns is 5 in Figure 6(a).

The pattern in certain floor might include one or more basic patterns. For example, $D3F3$ is composed of three different basic patterns shown in Figure 7. When X equals 3, the corresponding Y includes 1, 4 and 7 as shown in Figure 7(a). It can be concluded that $D3F3$ is composed by $D1$ (yellow), $D4$ (green) ,and $D7$ (blue) patterns shown in Figure 7(b). It can be expressed as $D3F3 = D1F1{+}D4F1{+}D7F1$. When X equals 6, the corresponding Y includes 2, 5 and 8, the equation can be expressed as $D3F6 = D2F1 + D5F1 + D8F1$. Similar composition in basic patterns also occurs in $D3F6$, $D6F3$, $D6F6$, $D9F3$, $D9F6$, and $D9F9$. $D9F9$ is composed by all basic patterns with digit 9.

Vedic square indicates not only the variation rule of digits patterns but also column and row on different floors in 3-D space. For example, the order of

column and row order on $F2$ are multiplying $F1$ by 2, which is equal to the number on the second column ($C2$) of $F1$, which is 2, 4, 6, 8, 1, 3, 5, 7, 9. First column ($C1$) on $F2$ is equal to $C2$ on $F1$, the relation can be expressed as $C1F2 = C2F1$. Columns and rows on specific floors follow this characteristic. To check whether h^{th} column (Ch) on i^{th} floor (Fi) is identical to j^{th} column (Cj) on k^{th} floor (Fk), the following equation is used to identify:

$$\text{If } D(hi) = D(jk), \text{ then } ChFi = CjFk. \tag{6}$$

When k=1, Cj, which represents the corresponding basic column of $ChFi$, can be identified.

This rule can also be applied to identify the order of floors in multi-dimensional space. For instance, there are 9 digital root cubes assumed in 4-D space. These 9 cubes are composed of multiplying vedic cube by 1 to 9. The value of second cube is multiplying digits of vedic cube by 2 and processes to digital root operation. The order of floors in second cube is $F2$, $F4$, $F6$, $F8$, $F1$, $F3$, $F5$, $F7$, $F9$ in vedic cube. The rule order of floors can be indicated from the column number of vedic square. The numbers of column on vedic square are very important basis for analyzing multi-dimensional space. In fact, variations from point to point, column to column, plane to plane, and cube to cube all possess similar rule. Noted that rules are different in the equation (5) of digital root patterns on specific floors.

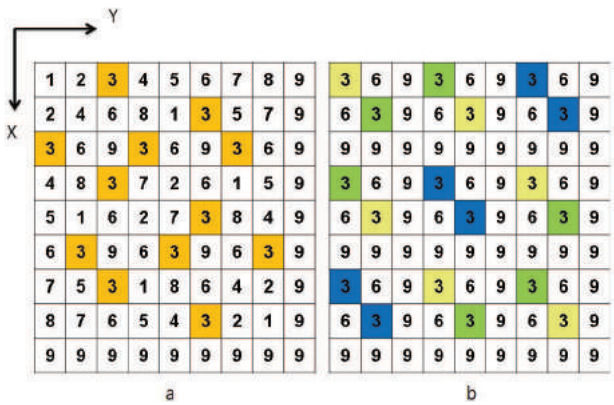

Figure 7: $D3F3$ is composed of three different basic patterns. (a) When X equals to 3, the corresponding Y is 1, 4 and 7, that means $D3F3$ is composed of $D1$, $D4$ and $D7$. And when X equals to 6, the corresponding Y is 2, 5 and 8. (b) $D3F3$ is composed of $D1$ (yellow), $D4$ (green) and $D7$ (blue) patterns.

3.4 Compensation of Patterns

This paragraph explains why patterns mirror each other along vertical line when digits summation in 9. There is a common geometric center for digit 1 to digit 8 (group A and B), that is point (4.5, 4.5, 4.5). In order to explain the symmetric characteristics of patterns, this part only discusses from digit 1 to digit 8 on both X and Y-axis. Figure 8(a) shows a diagonal inclining from left to right, which is

the main diagonal $X = Y$. Similarly, Figure 8(b) shows the other symmetric line inclining from right to left, which is the secondary diagonal $X + Y = 9$. Digits mirror each other along the main diagonal. In multiplication table, multiplying X by Y equals to multiplying Y by X, which can explain why digits mirror each other along the main diagonal. Furthermore, digits also mirror each other along secondary diagonal shown in Figure 8(b).
Before explaining the secondary diagonal, the basic operational rule of digital root should be clarified. In general, there are several basic operational rules of digital root, including addition rule:

$$D(X + Y) = D(D(X) + D(Y)). \tag{7}$$

Whether or not it can be applied in subtraction rule is another interesting topic. For example, 22 minus 15 equals 7, if their individual digital roots are calculated first, the result will be -2, which is a negative digital root. Calculation result for two equations should result in the same calculation outcome as $D(-2) = D(7) = 7$, because both -2 and 7 have the same remainder 7 when divided by 9 in modular arithmetic, which can be written as follow :

$$-2 \equiv 7 \pmod 9. \tag{8}$$

Ghannam (2012) assumes that $D(-51) = D(6) = 6$, and suggests ignoring the negative sign of the integer [9]. The digital root of a negative integer is calculated by adding it with multiple of 9 until the new number ranges from 1 to 9. The reason is because the digital root of an integer will remain the same if it adds or minuses the multiple of 9. Therefore, the digital root of -51 should be rewrite as follows:

$$D(-51) = D(-6) = D(3) = 3. \tag{9}$$

To explain the concept of the digital root of negative integer, digit 1 to 8 in vedic square are replaced by -8 to -1 in Y-axis, while X remains the same, see Figure 8(b). The original secondary diagonal becomes main diagonal. The characteristic of digit 8 mirroring each other along secondary diagonal is exactly like digit 1 mirroring along main diagonal. That can explain why two patterns mirror each other along vertical line when the digits summation is 9. It is important to note that this research only focuses on discussing digital root of positive integers. Negative digital root is used to help readers understand the symmetry in patterns, and to clarify the proper operation of negative digital root.

Here is another explanation why value of new coordinate point is identical to the original coordinate point $P(X, Y)$ from algebraic perspective. Value of any new coordinate point $P^*(9-Y, 9-X)$, which is the projection point of (X, Y) to secondary diagonal, is $D(P)$ in vedic square, and the difference of value between $D(P^*)$ and $D(P)$ is multiple of 9, which is shown as follows:

$$D(P^*) - D(P) = (81 - 9X - 9Y + XY) - (XY) = 81 - 9X - 9Y = 9k, k \in Z. \tag{10}$$

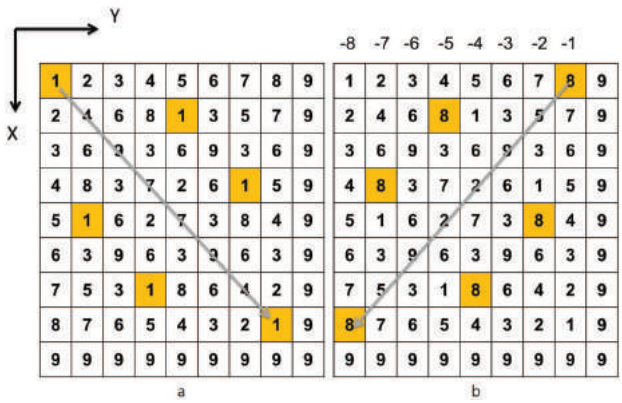

Figure 8: Digits mirror each other along the main and secondary diagonals on the vedic square. (a) Digit 1 mirrors each other along the main diagonal. (b) Digit 1 to 8 in vedic square is replaced by -8 to -1 in Y-axis, while X remains the same. The original secondary diagonal becomes main diagonal. The characteristic of digit 8 mirroring each other along secondary diagonal is exactly like digit 1 mirroring along main diagonal.

If value of the ninth column ($C9$) and the ninth row mirror along the secondary diagonal, the new points will become $(9-Y, 0)$, and $(0, 9-X)$, respectively. The two group of points are outside the range of vedic square. In order to maintain the consistency and symmetric characteristic of patterns, this research mainly considers from digit 1 to digit 8 on all three axes in 3-D space. However, for the recreational reason, we still provide digit 9 scattering plot with different boundary conditions in the appendices.

Floor method is used to analyze the characteristics on each floor and to identify the correlation with vedic square. However, it is important to discover those unseen pattern from a 3-D perspective. Therefore, we develop another methodology to analyze vedic cube and the digital root patterns in 3-D space.

3.5 Symmetric plane method

We use the second method to decompose vedic cube by two symmetric planes: Main symmetric planes and Secondary symmetric planes. Main symmetric planes (MSP) contain plane $X = Y$, $Y = Z$, and $X = Z$, each of them divides vedic cube into two grey blocks as shown in Figure 9(a). Secondary symmetric planes (SSP) contain $X + Y$=9, $Y + Z$=9, and $X + Z$=9, each of them also divides vedic cube into two grey blocks as shown in Figure 9(b). In both Figure 9(a) and 9(b), every grey block can mirror once to become vedic cube. It has nothing to do with choosing which side of the block as symmetric plane. Also, vedic cube can be decomposed into four prisms by MSP and SSP on $X - Y$, $Y - Z$, and $X - Z$ planes. The base of the prism is an isosceles right triangle with area equal to one-fourth of the square. To observe the digital root patterns in 3-D space, these blocks are intersected and analyzed using MSP and SSP within boundary conditions.

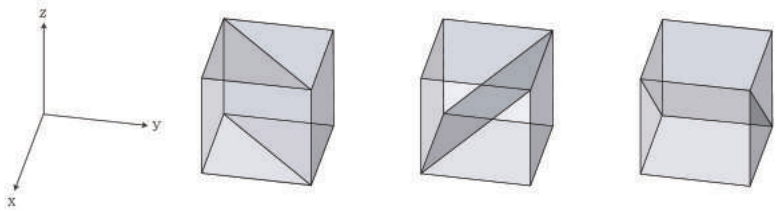

(a)

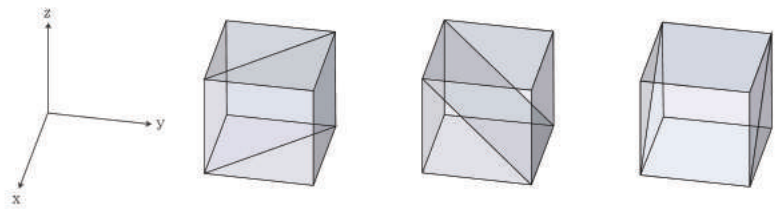

(b)

Figure 9: Decomposing vedic cube by main and secondary symmetric planes. (a) Main symmetric planes (MSP) contains plane $X = Y$, $Y = Z$, and $X = Z$, each of them divides vedic cube into two grey blocks (b) Secondary symmetric planes (SSP) contains $X + Y = 9$, $Y + Z = 9$, and $X + Z = 9$, each of them also divides vedic cube into two grey blocks.

Figure 10 shows segmentation result of MSP contains six congruent tetrahedrons (orthoscheme), each of them is also called birectangular tetrahedron which includes two right angles. In this study, birectangular tetrahedron is named MSP unit tetrahedron. The volume of a tetrahedron unit is one-sixth of the cube. It can mirror three times along $X = Y$, $Y = Z$, and $X = Z$ plane to become the initial cube. The intersection of MSP is found out to be space diagonal line $X = Y = Z$, it is reasonable to conclude that vedic cube is separated into six blocks by MSP.

The segmentation results of SSP are two congruent hexahedra and six congruent tetrahedrons. They are named as SSP unit hexahedron and SSP unit tetrahedron, respectively. Volume of a SSP unit hexahedron and a tetrahedron are one-fourth of the cube, and one-twelve of the cube, respectively. The intersection of SSP is a point, the central point of vedic cube (4.5, 4.5, 4.5). The intersection point indicates the reason why vedic cube is separated by SSP into eight blocks as shown in Figure 11. It is important to note that volume of each block is not exactly the same.

The final step is to analyze the intersection separated by both MSP and SSP, and the segmentation result is 24 congruent tetrahedrons. It is known as Goursat tetrahedron, or trirectangular tetrahedron which includes three right angles in a vertex. The Schlfli symbol is

$$\begin{bmatrix} 3 \\ 4 \\ 3 \end{bmatrix}$$

in Coxeter group [8]. It is named unit tetrahedron of vedic cube (UTVC) in this study. The base of UTVC is a right triangle with area occupying one-fourth of the square. The height is half of the length, and the volume is 1/24 of vedic cube as shown in Figure 12.

For the MSP unit tetrahedron, it is separated into four congruent UTVCs by the boundary conditions of SSP. There are mainly two cases for SSP unit hexahedron and SSP unit tetrahedron. The first case is six UTVCs separated by SSP unit hexahedron; the second case is two UTVCs separated by SSP unit tetrahedron, with both within the boundary condition of MSP.

UTVC can mirror six times along MSP and SSP to become the vedic cube, only points of digit 1, 2, 3 and 4 of UTVC have to be listed. Then original complicated digital root patterns in 3-D space can therefore be simplified. The symmetric plane method reduces the complexity of vedic cube and allows the basic element in vedic cube to be easily recognized.

Points in UTVC of digit 1, 2, 3 and 4 within boundary conditions ($X \leq Y$, $Y \leq Z$, $X \leq Z$, $X+Y \leq 9$, $Y+Z \leq 9$, $X+Z \leq 9$) are listed in Table 1. Points on the boundary are shared by several UTVCs. Points in UTVCs can be used to reflect others points by MSP and SSP.

We invite readers to execute the "*digit_3D*" program provided in appendices A.1 to observe the digital root patterns from different boundary conditions, floors and views and have fun.

Figure A-2 to A-6 of appendices show the result of specific digit scatter in vedic cube with corresponding boundary conditions by *digit_3D*. BC1, BC2, BC3 and BC4 represent boundary conditions ($X \leq Y$, $Y \leq Z$, $X \leq Z$, MSP unit tetrahedron), ($X+Y \leq 9$, $Y+Z \leq 9$, $X+Z \leq 9$, SSP unit hexahedron), ($X+Y \leq 9$, $Y+Z \geq 9$, $X+Z \geq 9$, SSP unit tetrahedron) and ($X \leq Y$, $Y \leq Z$, $X \leq Z$, $X+Y \leq 9$, $Y+Z \leq 9$, $X+Z \leq 9$, UTVC), respectively. To be noted, digit 9 is not symmetric along SSP in the vedic cube, which is mentioned in section 3.4.

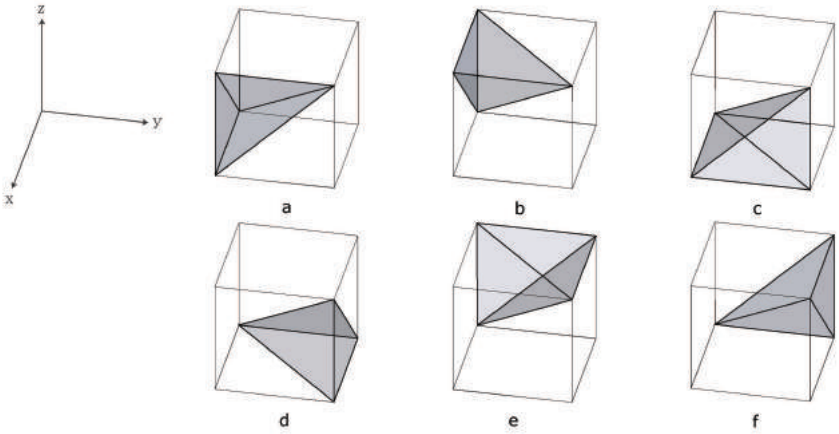

Figure 10: Segmentation result of main symmetric planes (MSP). There are six congruent tetrahedrons (orthoscheme), one of which is also called birectangular tetrahedron including two right angles. Volume of a tetrahedron is one-sixth of the cube. It is called MSP unit tetrahedron in this research. Corresponding boundary conditions of each block are (a) $X \geq Y$, $Y \leq Z$, $X \geq Z$; (b) $X \geq Y$, $Y \geq Z$, $X \leq Z$; (c) $X \geq Y$, $Y \geq Z$, $X \geq Z$; (d) $X \leq Y$, $Y \geq Z$, $X \geq Z$; (e) $X \leq Y$, $Y \leq Z$, $X \leq Z$; (f) $X \leq Y$, $Y \geq Z$, $X \leq Z$.

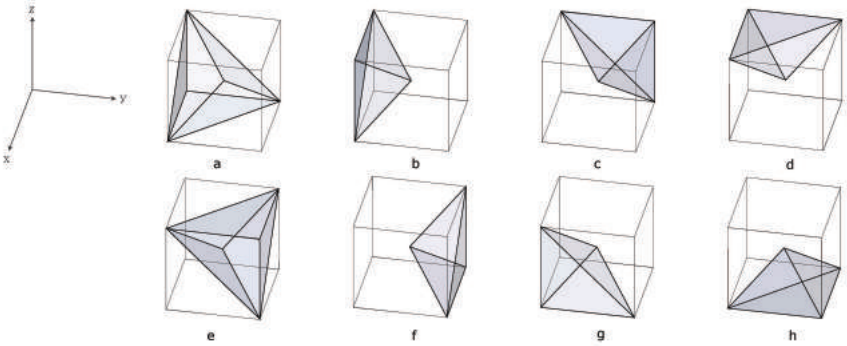

Figure 11: Segmentation result of secondary symmetric planes (SSP). There are two SSP unit hexahedron and six SSP unit tetrahedron, corresponding volume are one-fourth and one-twelve. Corresponding boundary conditions of each block are (a)$X + Y \leq 9$, $Y + Z \leq 9$, $X + Z \leq 9$; (b)$X + Y \leq 9$, $Y + Z \leq 9$, $X + Z \geq 9$; (c)$X + Y \leq 9$, $Y + Z \geq 9$, $X + Z \leq 9$; (d)$X + Y \leq 9$, $Y + Z \geq 9$, $X + Z \geq 9$; (e)$X + Y \geq 9$, $Y + Z \geq 9$, $X + Z \geq 9$; (f)$X + Y \geq 9$, $Y + Z \geq 9$, $X + Z \leq 9$; (g)$X + Y \geq 9$, $Y + Z \leq 9$, $X + Z \geq 9$; (h)$X + Y \geq 9$, $Y + Z \leq 9$, $X + Z \leq 9$.

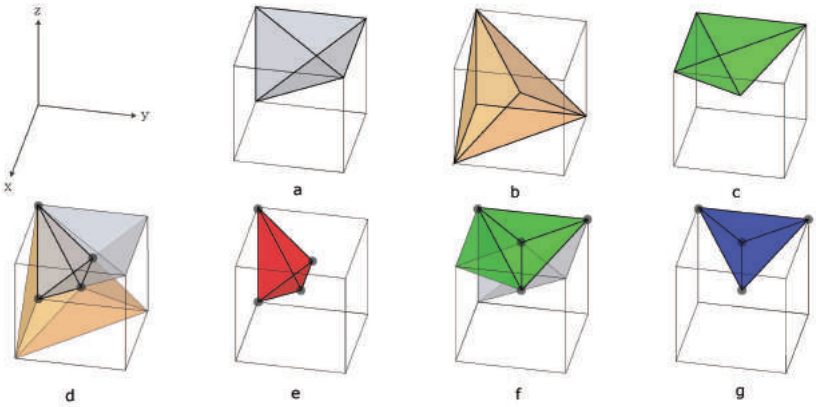

Figure 12: Intersection of the blocks separated by MSP and SSP. (a) MSP unit tetrahedron identical Figure 10(e). (b) SSP unit hexahedron is identical to Figure 11(a). (c) SSP unit tetrahedron is identical to Figure 11(d). (d) Union of part a and b. (e) Intersection of part a and b (f) Union of part a and c. (g) Intersection of part a and c. The final segmentation result is 24 congruent tetrahedrons, part e and g are two of them.

Table 1: Points in the Unit tetrahedron of vedic cube (UTVC).(B.C.: $X \leq Y$, $Y \leq Z$, $X \leq Z$, $X + Y \leq 9$, $Y + Z \leq 9$, $X + Z \leq 9$)

Digit 1	Digit 2	Digit 3	Digit 4
(1,1,1)	(1,1,2)	(1,1,3)	(1,2,2)
(1,2,5)	(1,4,5)	(2,2,3)	(1,1,4)
(2,2,7)	(2,2,5)	(1,3,4)	(2,4,5)
(4,4,4)		(3,4,4)	
		(2,3,5)	
		(1,2,6)	

3.6 Extra findings

In Table 1, there are extra findings in observing points in the UTVC which are not located within the boundary. Those points of digit 1, 2, 4 are (1,2,5), (1,4,5), (2,4,5), respectively. The three points form a right triangle with lengths of 1, 2, and $\sqrt{5}$. Furthermore, points of digit 3 are (1,3,4), (2,3,5), (1,2,6), they also form a right triangle with side length $\sqrt{2}$, $\sqrt{3}$, and $\sqrt{5}$.

3.7 Six coordinate points

Six coordinate points (X, Y), $(2X, 5Y)$, $(4X, 7Y)$, $(5X, 2Y)$, $(7X, 4Y)$, $(8X, 8Y)$ in Figure 6(b) can be used to find other five points with same digit. For example, the digital root of (4,8) is 5 in vedic square , and the other five points would be (8,4), (7,2), (2,7), (1,5) ,and (5,1) due to having the same digital root operation results listed as follows:

$$D(X,Y) = D(2X,5Y) = D(4X,7Y) = D(5X,2Y) = D(7X,4Y) = D(8X,8Y). \tag{11}$$

The same rule can also be applied in 3-D space. For instance, point (5,1) indicates that pattern of digit 5 on $F1$ can be written as $D5F1$, which is also the pattern to the other five points (1,5), (2,7), (7,2), (8,4), (4,8). Take point (4,8) to implement the rule, position of digit 4 on $F1$(vedic square) will be the same as digit 5 on $F8$.

There are two more groups for digit 3 and 6, the first group contains $(X,4Y)$, $(2X,2Y)$, $(4X,Y)$, $(5X,8Y)$, $(7X,7Y)$, and $(8X,5Y)$; the second group contains $(X,7Y)$, $(2X,8Y)$, $(4X,4Y)$, $(5X,5Y)$, $(7X,Y)$, $(8X,2Y)$. For the first group, the digital root operation by multiplying coefficient of X by Y are 4, which yields

$$D(X,4Y) = D(4\times D(X,Y)) = D((3+1)\times D(X,Y)) = D(9+D(X,Y)) = D(X,Y). \tag{12}$$

The equation also applies when the product of X and Y coefficient is 7. However, the six points found from these two groups are identical to the original group. There is a difference between total number of group B (12 numbers of each) and group A (6 numbers) in vedic square, because the points produced by group B mirroring along the diagonal $X = Y$ are different from the six coordinate points. That is the reason why 12 numbers are within each one of group B in vedic square.

The geometric indication of six groups is that we could find a new coordinate point by moving the multiple of coefficient from original X coordinate position on the X axis. The coordinate point on Y axis can also be found by the same rule.

The main advantage of six coordinate points method is convenient to find the other five coordinate points from a single known coordinate point. It is impossible to mirror all points along diagonals from a single point because there must be some points locating on one of two diagonals, at least two coordinate points are required to mirror all the points with the same digital root on a plane.

4 Conclusion

This paper investigates the digital root patterns by adopting two different approaches in the 3-D space. Simplification in vedic cube is very important to understand characteristics of digital root patterns in 3-D space. From floor method, characteristics of digital root patterns of 2-D space can be applied to 3-D space, including distribution regularities of basic pattern, columns on the different floors, and specific digital root patterns on specific floors which might

be composed of several basic patterns. To sum up, 2-D space (vedic square) can be seen as a basic reference for 3-D space (vedic cube) and 4-D space similarly. Symmetric plane method greatly reduces the complexity of vedic cube and it can be used to find out the digital root patterns of 3-D space, reducing the limitation of only analyzing the correlation between 2-D spaces. The discovery pattern of vedic cube expands the geometric patterns from 2-D space to 3-D space, even for multi-dimensional space. Digital root patterns of 3-D space are the mysteries formed by the nature. Except pure mathematics research, this study can be applied as a rule to develop an algorithm to discover textile patterns in 3-D space, molecular crystals, architecture, space, and artistic fields.

5 Acknowledgements

Thanks to Ya-Chi Lee, Ching-Yen Lin, Meng-Shen Kan, Chu-Han Yen, Yi-Hua Yu, Prof. Hsiao-Wen Wang and Prof. Jian-Ping Suen.

References

[1] Abas, S. J., Salman, A. S. *Symmetries of Islamic geometrical patterns*, World Scientific, Singapore, 1995.

[2] Balmond, C. *Number 9*, Prestel, Munich, 1998.

[3] Balmond, C. *Element*, Prestel, Munich, 2007.

[4] Balmond, C. *Crossover*, Prestel, Munich, 2013.

[5] Balmond Studio. 2012. `http://www.balmondstudio.co.in/pavilions_images/serp2002_3.jpg`

[6] Balmond Studio. 2013. `http://www.balmondstudio.com/work/serpentine-pavilion-2002/`

[7] Bunyard, D., Brine, A. "Islamic art: Vedic square", *Micromath*, 1988.

[8] Coxeter, H. S. M. *Regular Polytopes*, Dover, New York, 1973.

[9] Ghannam, T. *The Mystery of Numbers: Revealed Through Their Digital Root (2nd Edition): Unraveling the Hidden Design of the Universe through The Digital Root of Numbers*, CreateSpace, North Charleston, SC, USA, 2012.

[10] Jones, L. "Mathematics and Islamic art", *Mathematics in School*, 18(4), 32–35, 1989.

[11] Lu, P. J., Steinhardt, P. J. "Decagonal and Quasi-Crystalline Tilings in Medieval Islamic Architecture", *Science*, 315(5815), 1106–1110, 2007.

[12] The British Library Board. *Mamluk Qur'an*, 2015. `http://www.bl.uk/onlinegallery/sacredtexts/mamlukquran.html`

Appendices

A.1 Digital root patterns visualization "*digit_3D*" program

Please refer to the following url to access the "*digit_3D*" program (current version:1.5).

`http://140.116.77.14/ecowater/member/102_CYLin.htm`

A.2 Points list

Table A-1: Points of digit 1, 2, 3 and 4 in four UTVCs with corresponding boundary conditions.

	$X \le Y$, $Y \le Z$, $X \le Z$			
	$X+Y \le 9$ $Y+Z \le 9$ $X+Z \le 9$	$X+Y \ge 9$ $Y+Z \ge 9$ $X+Z \ge 9$	$X+Y \le 9$ $Y+Z \ge 9$ $X+Z \le 9$	$X+Y \ge 9$ $Y+Z \ge 9$ $X+Z \ge 9$
Digit 1	(1,1,1)	(1,8,8)	(1,8,8)	(1,8,8)
	(1,2,5)	(5,7,8)	(1,4,7)	(2,4,8)
	(2,2,7)	(7,7,7)	(2,2,7)	(2,2,7)
	(4,4,4)	(4,5,5)	(4,5,5)	(4,5,5)
Digit 2	(1,1,2)	(2,8,8)	(1,7,8)	(2,8,8)
	(1,4,5)	(5,5,8)	(1,4,5)	(4,4,8)
	(2,2,5)	(5,7,7)	(2,4,7)	(2,4,7)
Digit 3	(1,1,3)	(3,8,8)	(1,6,8)	(1,6,8)
	(1,2,6)	(6,7,8)	(1,3,7)	(2,3,8)
	(1,3,4)	(4,6,8)	(1,5,6)	(3,5,8)
	(2,2,3)	(3,7,7)	(2,6,7)	(2,6,7)
	(2,3,5)	(5,6,7)	(3,4,7)	(3,4,7)
	(3,4,4)	(4,5,6)	(3,5,5)	(4,5,6)
Digit 4	(1,1,4)	(4,8,8)	(1,5,8)	(1,5,8)
	(1,2,2)	(2,7,8)	(1,7,7)	(2,7,8)
	(2,4,5)	(5,5,7)	(2,4,5)	(4,4,7)

A.3 Scatter plot

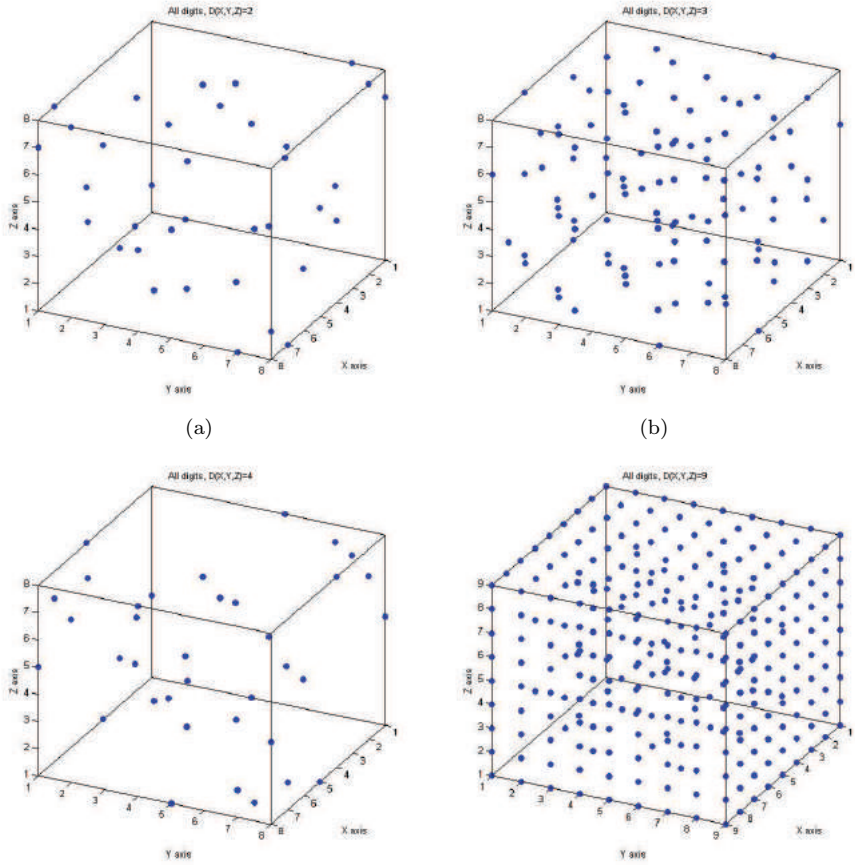

(a) (b)

(c) (d)

Figure A-1: Points of digit scatter in vedic cube. (a) digit 2 (b) digit 3 (c) digit 4 (d) digit 9.

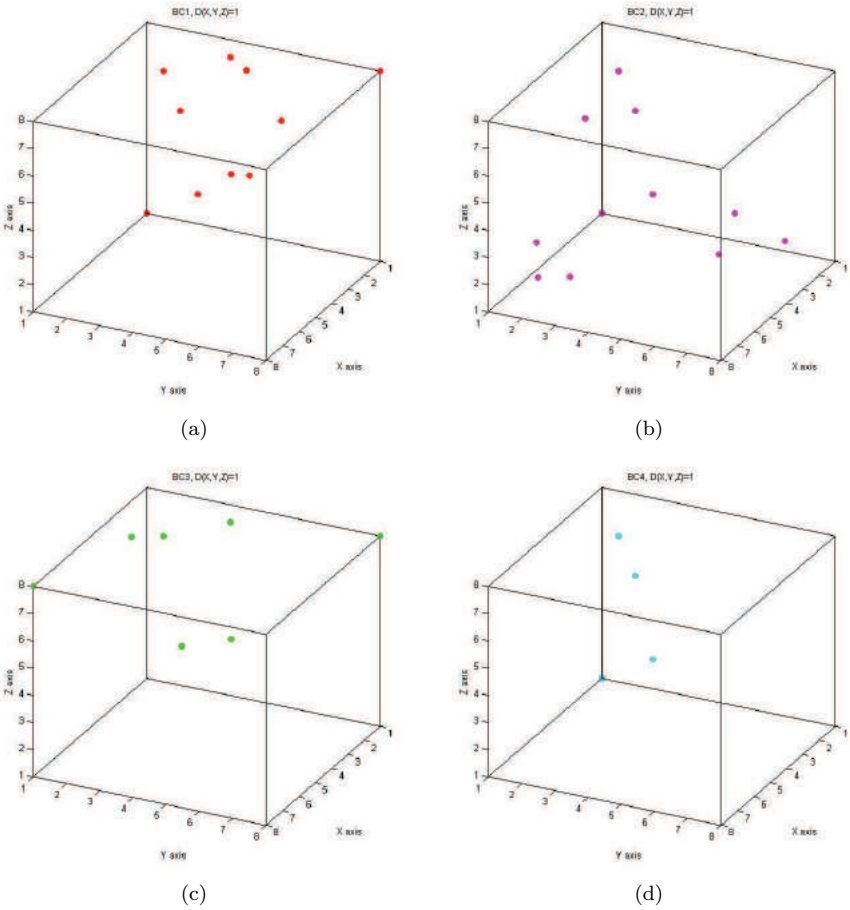

Figure A-2: Points of digit 1 scatter in vedic cube with corresponding boundary conditions (a) BC1 (b) BC2 (c) BC3 (d) BC4.

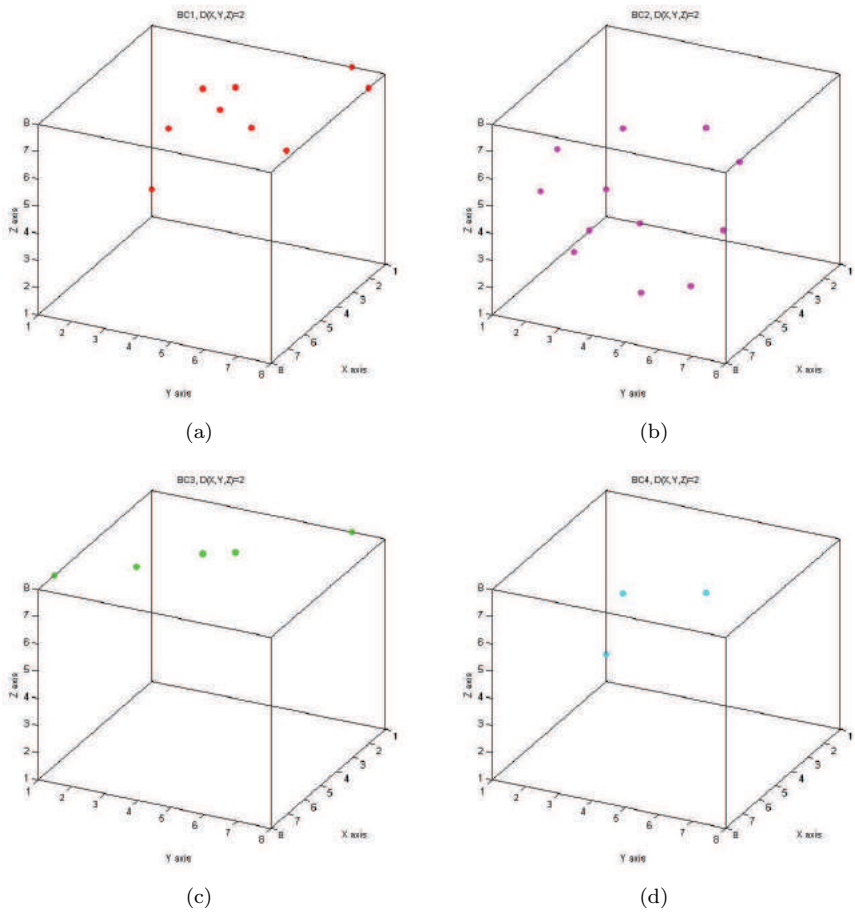

Figure A-3: Points of digit 2 scatter in vedic cube with corresponding boundary conditions (a) BC1 (b) BC2 (c) BC3 (d) BC4.

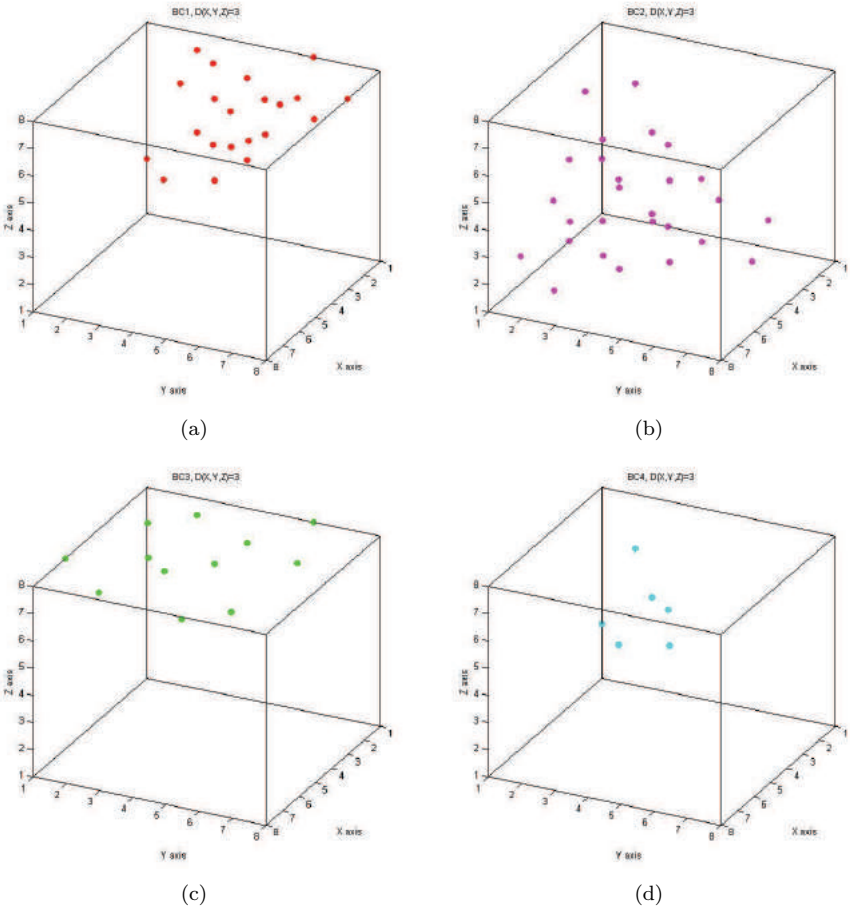

Figure A-4: Points of digit 3 scatter in vedic cube with corresponding boundary conditions (a) BC1 (b) BC2 (c) BC3 (d) BC4.

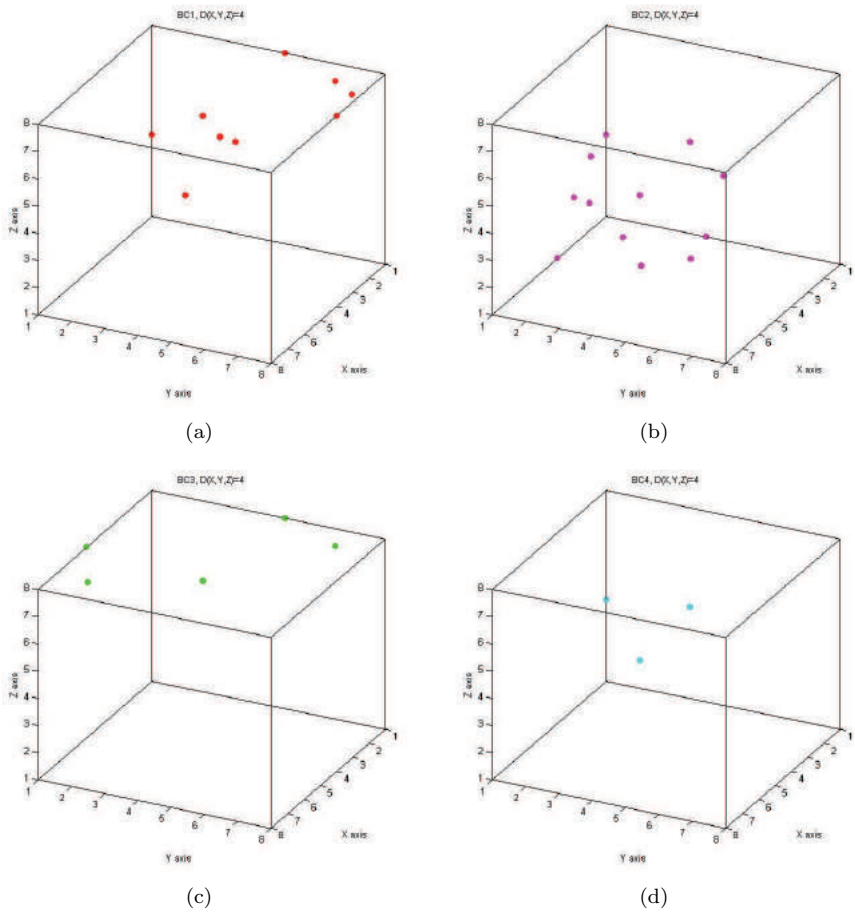

Figure A-5: Points of digit 4 scatter in vedic cube with corresponding boundary conditions (a) BC1 (b) BC2 (c) BC3 (d) BC4.

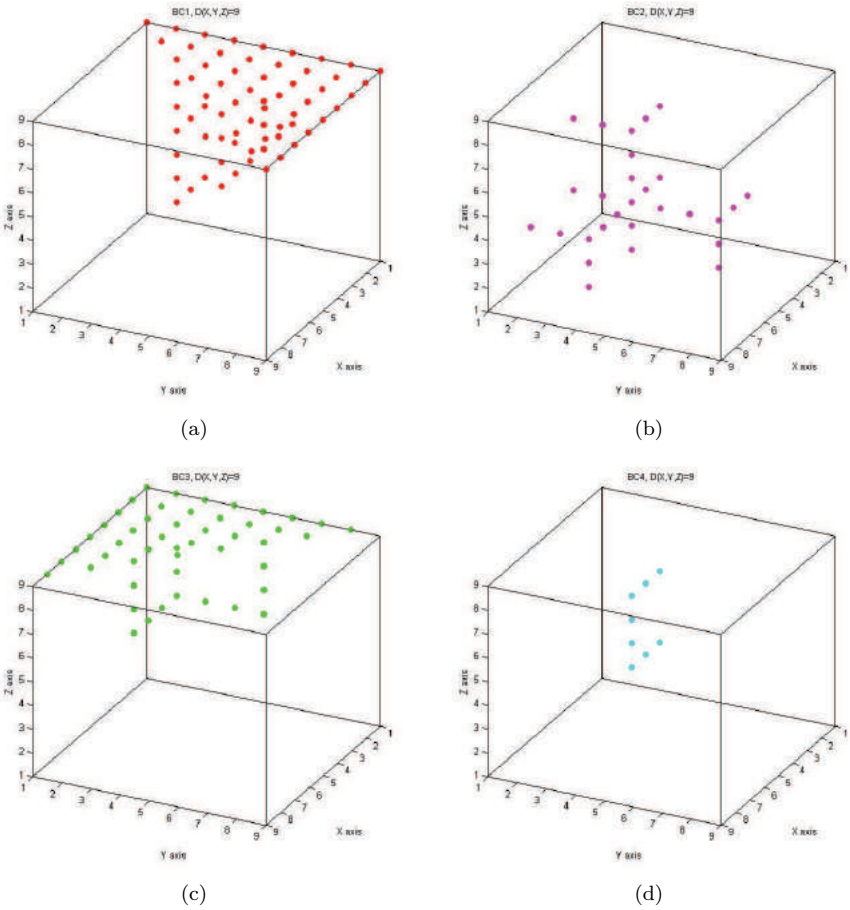

Figure A-6: Points of digit 9 scatter in vedic cube with corresponding boundary conditions (a) BC1 (b) BC2 (c) BC3 (d) BC4.

Mathematics and Arts

Allégorie de la Géométrie
A MATHEMATICAL INTERPRETATION

Alda Carvalho, Carlos Pereira dos Santos, Jorge Nuno Silva
ISEL & Cemapre-ISEG, CEAFEL-UL, University of Lisbon
acarvalho@adm.isel.pt cmfsantos@fc.ul.pt jnsilva@cal.berkeley.edu

Abstract: *In this work, we present a mathematical interpretation for the masterpiece* Allégorie de la Géométrie *(1649), painted by the French baroque artist Laurent de La Hyre (1606–1656).*

Keywords: Laurent de La Hyre, "Allégorie de la Géométrie", baroque art, mathematical interpretation, perspective.

Introduction

The main purpose of this text is to present a mathematical interpretation for the masterpiece *Allégorie de la Géométrie*, from a well-known series of paintings, *Les 7 arts libéraux*, by the French baroque artist Laurent de La Hyre (1606–1656).

Figure 1: *Allégorie de la Géométrie* (1649), oil on canvas.

Laurent de La Hyre painted the series *Les 7 arts libéraux* between 1649 and 1650 to decorate Gédéon Tallemant's residence. Tallemant was an adviser of Louis XIV (1638–1715). The king was 10 years old at the time of the commission. According to the artist's son, Philippe de La Hire (1640–1718), writing around 1690 [5],

> (...) une maison qui appartenoit autrefois a M. Tallemant, maistre des requestes, sept tableaux represéntant les sept arts liberaux qui font l'ornement d'une chambre.

Also, Guillet de Saint-Georges, a historiographer of the *Académie Royale de Peinture et de Sculpture*, mentioned that it was Laurent's work for the Capuchin church in the Marais which led to the commission for the "Seven Liberal Arts" in a house [2].

The seven liberal arts were seen as the crucial parts of learning, distinct from philosophy (knowledge) and manual arts (e.g., agriculture). They come from ancient Greece and have been depicted as women ever since. That is why geometry is personified by a woman in Laurent's painting.

As a general impression, *Allégorie de la Géométrie* shows rich color and nice forms (characteristic of Laurent's style). Geometry was personified as a young woman holding a compass and right angle in one hand and a "mysterious" sheet inscribed with mathematical diagrams in the other. She is surrounded by monuments, a globe, pyramids, a sphinx, all in an Egyptian-Greek athmosphere. The first obvious ideas suggest the opposites practice/theory and concrete/abstract (somehow related to ancient Greece/ancient Egypt) and for the impeccable technique (rigorous perspective). The dualities concrete-abstract and practice-theory strike us as *they go hand in hand* with the Egypt-Greece visual context. Accordingly, somehow, the theoretical mathematical results should be related to the concrete situations displayed in the painting.

Laurent's series was dispersed sometime between 1760 and 1793. At present we know nine paintings that belonged to the original group [9]. The *Allégorie de la Géométrie* was recently acquired by Fine Arts Museums of San Francisco. In early 2014, the work was valued between USD$800,000 and 1.2 million dollars [6].

Relevant facts about Laurent de La Hyre

Laurent de La Hyre, born in a bourgeois milieu, received a high-level education, having been a student of the painter Georges Lallemant (1575–1636). De La Hyre is well-known for his paintings incorporating scenes from classical antiquity. He regularly represented ruins backgrounds based on a very careful design: *Allégorie de la Géométrie* is one such example. Laurent's home was a stimulating place, receiving visits of prominent artists, scientists, and mathematicians: our analysis is consistent with this fact. Mathematics and geometry played an important role in Laurent's life. The great mathematician Girard Desargues (1591–1661), one of the founders of projective geometry, was among his regular

visitors. One source for projective geometry was the theory of perspective, very important for the development presented in the next section. In that theory, a horizon line is a theoretical line that represents the eye level of the observer, vanishing points are points where parallel lines converge, vertical lines maintain the verticality in the paintings, etc [7]. Laurent de La Hyre was an expert using these geometric concepts in his paintings. Euclidean geometry and theory of perspective were also important for Laurent's descendants, perhaps influenced by the environment they lived in as children. Philippe de La Hire (1640–1718), Laurent's son, was a mathematician and astronomer; his works on conic sections and epicycloids were based on the teaching of Desargues, of whom he was the favorite pupil. Gabriel-Philippe de La Hire (1677–1719), Philippe's son and Laurent's grandson, was also a mathematician. These remarks suggest that the family was very mathematicaly minded.

A Mathematical Interpretation for the *Allégorie de la Géométrie*

First, we list some key ideas that can be found in other published interpretations (all inspired by [8]):

> Of all the works in the series, *Allégorie de la Géométrie* perhaps held the greatest personal significance for the artist, since knowledge of the discipline, in the form of perspective, was crucial for the practice of painting at the time. In the late 1630s, De la Hyre studied with the mathematician Girard Desargues, who is considered one of the founders of projective geometry [6].

> In the center of the composition sits the embodiment of geometry, leaning on a block of marble. In her right hand is a sheet of paper with a diagram of the golden section and three Euclidean proofs, which she holds up for the viewer to see. In her left hand is a compass and a right angle, tools of a mathematician and geometer. Surrounding her are references to the practical applications of geometry, beginning at the left with a painting set on an easel, the painter's palette and brushes affixed below. The globe next to it stands for the earth, but also is a product of geometry, as geometry underpins the process of map making. The snake above is an attribute for the goddess Ceres, an older representation of the earth. (...) At the right is a sphinx, representing Egypt, where an early form of geometry was invented, but the large crack in its back represents the flaws in the Egyptian approach; it was not until the advent of Euclid that modern geometry was developed [6].

> A relief is carved on the side of a tomb; the sacrificial scene may carry a hidden meaning. At the right sits a sphinx that symbolically represents Egypt, where an early form of geometry was developed. The painting relays the idea that the Egyptians developed an imperfect and inferior geometry based on practical necessity compared Greek geometry, which was valued as abstract thought and pure learning [1].

In the following interpretation, the idea that "the Egyptians developed an *imperfect and inferior geometry* based on practical necessity compared Greek geometry" is replaced by the idea of *complementarity*; the idea of "a diagram of the golden section" is simply not true; the idea of "three Euclidean proofs, for the viewer to see" is much more sophisticated because the three results are really crucial *to understand the painting*; the idea of a "globe standing for the earth and also a product of geometry" is quite important and *it is related to one of the Euclidean proofs*; the idea of "greatest personal significance for the artist" because of "perspective, crucial for the practice of painting at the time" may be greatly expanded.

THE "MYSTERIOUS" SHEET OF PAPER

The young woman holds a "mysterious" sheet containing mathematical illustrations (Figure 2).

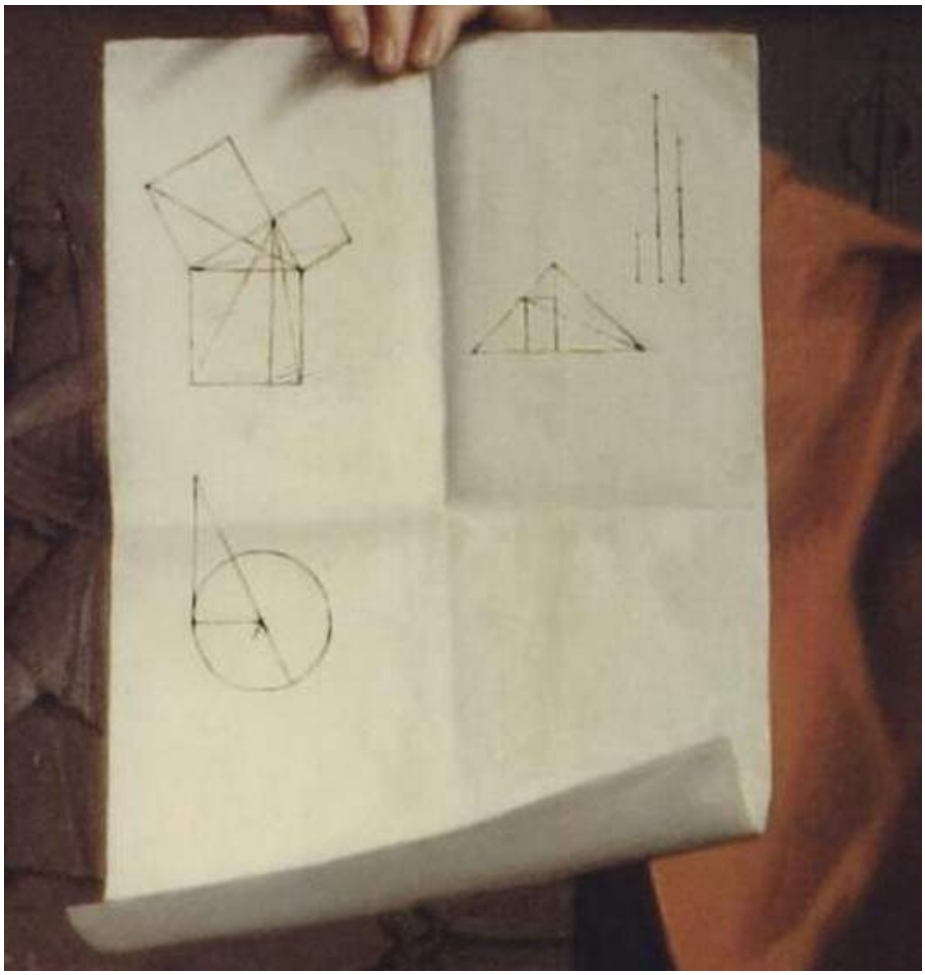

Figure 2: Mathematical diagrams.

For sure, the top-left diagram illustrates the famous Pythagorean Proposition (*Elements* I, 47, [3]), stating that, in a right triangle, the sum of the squares on the two legs equals the square on the hypotenuse (Figure 3).

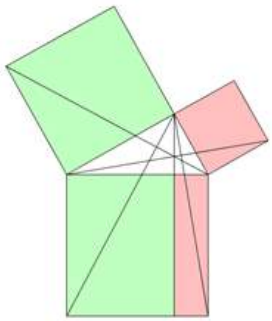

Figure 3: *Elements* I, 47.

In the painting, there are objects with right angles everywhere. Furthermore, the young woman holds a compass and a right angle on the other hand. But we think there are more hidden reasons for the Theorem's occurrence. Later, a possible use of the Pythagorean Theorem for the painting process will be presented.

The top-right diagram is very interesting. First of all, *it is not related to the golden ratio.* It is more likely to be the *Elements* II, 9 [3]:

If a straight line is cut into equal and unequal segments, then the sum of the squares on the unequal segments of the whole is double the sum of the square on the half and the square on the straight line between the points of section.

Let a segment $[AB]$ be cut into equal segments at C, and into unequal segments at D (Figure 4). Then, $\overline{AD}^2 + \overline{DB}^2 = 2(\overline{AC}^2 + \overline{CD}^2)$.

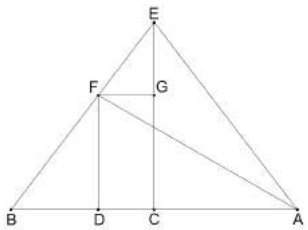

Figure 4: *Elements* II, 9.

The diagram for the proof is the same as the drawing exposed in the sheet of paper. That is the likely reason for the idea that *all diagrams* are related to Euclidean results. However, there is a big but. Proposition 9 is not related, in any way, to the atmosphere of the painting. It is much more logical to prove the following result:

Theorem 1. *Consider ABC, a isosceles triangle, D, the midpoint of $[AB]$ and E, the midpoint of $[DC]$. Let G be the intersection of AE with BC and H its perpendicular foot in $[AB]$. Then,*

$$\frac{\overline{GH}}{\overline{DE}} = \frac{4}{3}\cdot$$

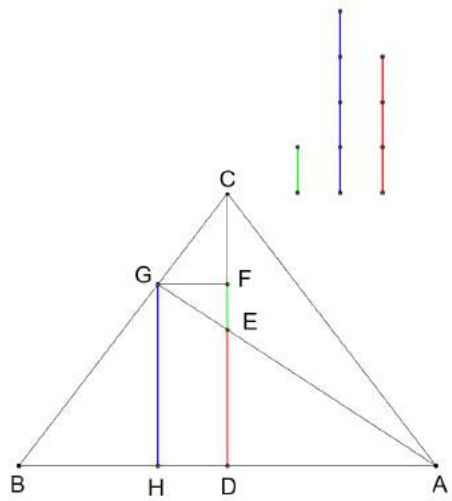

Figure 5: Four thirds rule.

Proof.

First,

$$\frac{\overline{CD}}{\overline{AD}} = \frac{\overline{CF}}{\overline{FG}} \Leftrightarrow \frac{2\times\overline{DE}}{\overline{AD}} = \frac{\overline{CE}-\overline{EF}}{\overline{FG}} \Leftrightarrow \frac{2\times\overline{DE}}{\overline{AD}} = \frac{\overline{DE}}{\overline{DH}} - \frac{\overline{EF}}{\overline{DH}}\cdot$$

Second,

$$\frac{\overline{EF}}{\overline{FG}} = \frac{\overline{DE}}{\overline{AD}} \Leftrightarrow \frac{\overline{EF}}{\overline{DH}} = \frac{\overline{DE}}{\overline{AD}}\cdot$$

Joining first and second,

$$\frac{2\times\overline{DE}}{\overline{AD}} = \frac{\overline{DE}}{\overline{DH}} - \frac{\overline{DE}}{\overline{AD}} \Leftrightarrow \frac{\overline{DH}}{\overline{AD}} = \frac{1}{3}\cdot$$

Finally,

$$\frac{\overline{GH}}{\overline{DH}+\overline{AD}} = \frac{\overline{DE}}{\overline{AD}} \Leftrightarrow \frac{\overline{GH}}{\overline{DE}} = \frac{\overline{DH}+\overline{AD}}{\overline{AD}} \Leftrightarrow \frac{\overline{GH}}{\overline{DE}} = 1 + \frac{\overline{DH}}{\overline{AD}} \Leftrightarrow \frac{\overline{GH}}{\overline{DE}} = \frac{4}{3}\cdot$$

□

What is interesting about this result is its generality: it works for *all* isosceles triangles. Moreover, it corresponds exactly to the diagram in the sheet of paper. We observe that the painting has several pyramids of *different shapes*. If someone wanted to make a tunnel from the ground, passing through a room in the center of a pyramid, this result would provide the location of the exit on the other side (Figure 6).

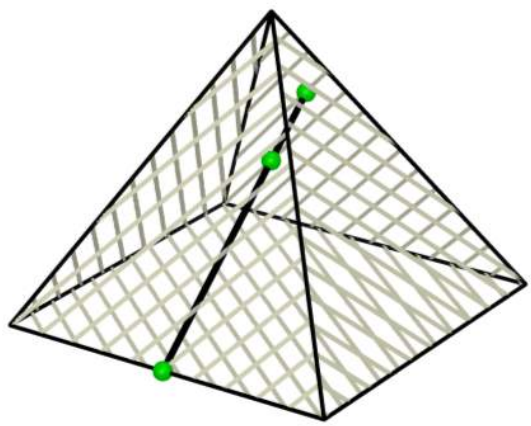

Figure 6: Pyramid.

Laurent de La Hyre did not have the modern knowledge about the interior of the Egyptian pyramids, their astronomical significance and construction methods. Nevertheless, apart from the fact that looting had been common practice for a long time, the existence of chambers, both interior and underground is old knowledge. For example, Herodotus (484–425 BC) mentioned

> (...) The aforesaid ten years went to the building of this road and of the underground chambers in the hill where the pyramids stand [4].

The use of mathematics in human buildings is a central issue in this Laurent's artwork. Egyptian pyramids in the background make it natural that Laurent de La Hyre may have thoughts about the architecture and the interior of the pyramids.

The bottom diagram is also interesting. *Elements* I, 32 [3] states that three interior angles of a triangle are equal to two right angles. Using that, the relation illustrated in the Figure 7 has a very easy proof.

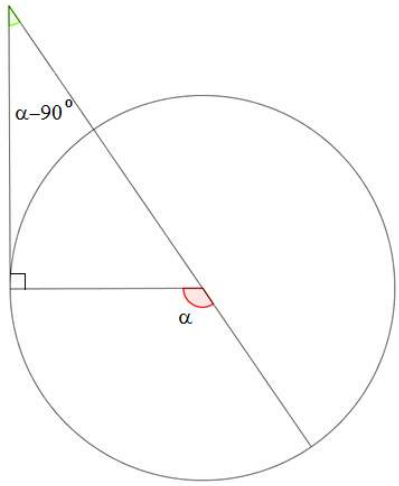

Figure 7: Bottom diagram.

Of course, the fundamental question is to know *why* that particular relation is there. If we contextualize we risk a guess (Figure 8).

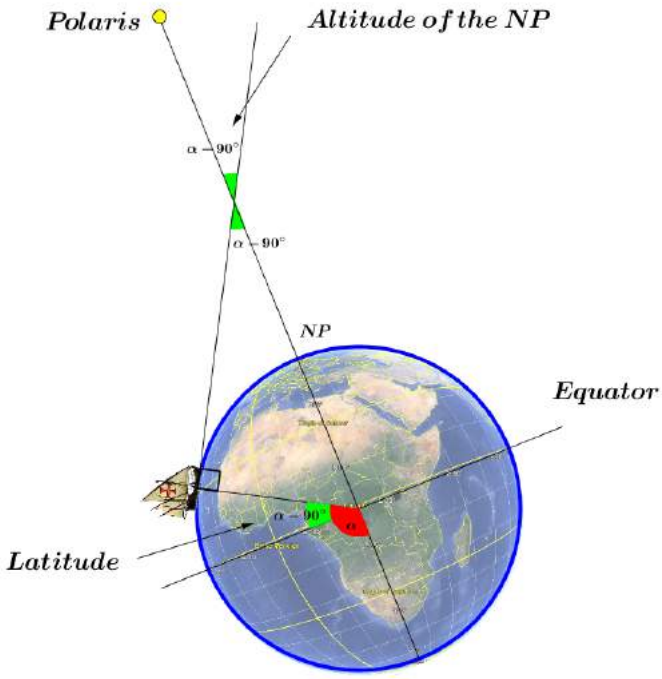

Figure 8: Latitude determination.

The result in question gives a direct argument for the fact that the altitude of the northern celestial pole is exactly the latitude. The globe, as well as Ceres' snake, draws attention to the use of geometry in surveying, navigation, map making, and so on. The chosen geometric relation is a concrete example of that use.

We observe that the Pythagorean theorem, the relation latitude/altitude of the northern pole and the Four thirds rule are general results, showing the incredible power of geometry, the main theme of the painting. The Pythagorean theorem holds for *all right triangles*; the relation latitude/altitude of the NP holds for *any place on Earth*, the Four thirds rule holds for *all isosceles triangles* (and, thus, for all pyramids). That strong power and generality of geometry is exactly what Laurent de La Hyre wanted to transmit in his masterpiece.

PERSPECTIVE

Laurent de La Hyre learned techniques on perspective from Girard Desargues. Basically, perspective is a representation, on a flat surface (canvas), of an image as it is seen by the observer's eye. Italian Renaissance painters, including Filippo Brunelleschi, Masaccio, Paolo Uccello, Piero della Francesca, and Luca Pacioli, studied perspective, incorporating it into their artworks. An important characteristic feature of perspective is that vanishing points are points where parallel lines converge. In we consider some obvious parallel lines (not the horizontal lines of the painting inside the painting!), we find that the head of the sphinx is a vanishing point (Figure 9).

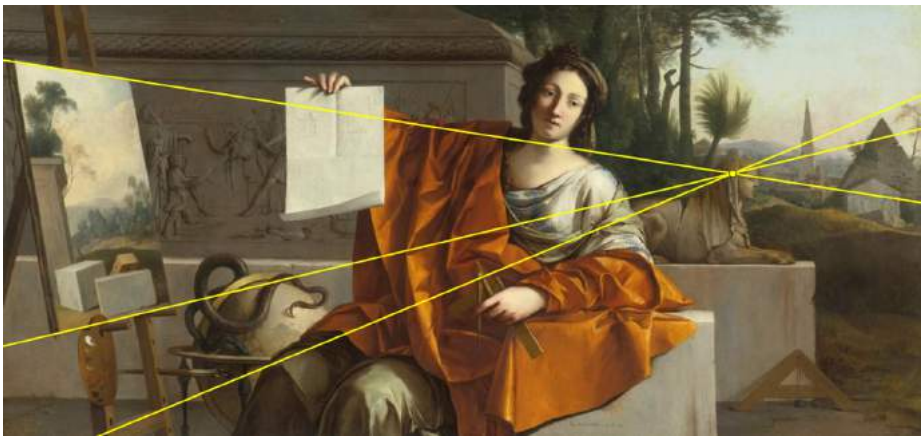

Figure 9: Head of the sphinx.

This fact is full of meaning. Everything takes place in the head of the sphinx, symbolizing the complementarity between ancient Greece and ancient Egypt and, more generally, between practical knowledge and mathematical theory. This makes even more sense considering that the sphinx is an important element of both Greek and Egyptian cultures.

Perspective arises as a self-referential piece. This hymn to geometry begs to be approached geometrically. The painting within the painting is a natural challenge. Its lack of human presence seems to tell us that the practical applications derived from mathematical theory enrich the world in an essential way.

We did some experiments to assess if the perspective within the perspective is accurate. Mathematically speaking, it is a composition of perspectives. Of course, it is almost impossible to know the exact perspective techniques used by the artist, but we can easily verify whether the perspective is rigorous. Notice that the cuboids are the easiest objects to represent. That reinforces the idea that one of the artist's purposes was to execute a composition of perspectives. After analyzing several possibilities (canvas and block dimensions, observer's position, block positions), we got the figure of the appendix 1 as a *possible* "inner painting". In Appendix 1, the observer lives in the painting world. Then, we studied the perspective made *with that possibility* (canvas dimensions, observer's position, height and inclination of the canvas) and we got the figure of the Appendix 2. In that case, the observer lives in our world and, as expected, his eye's level is the sphinx's head level. The matching is really impressive.

Observe that the inclination of the inner painting is an important parameter (our conclusion suggests $\alpha = 77°$). Because the heights are needed informations, maybe the artist used the diagram of the Figure 10. An easy application of the Pythagorean Theorem.

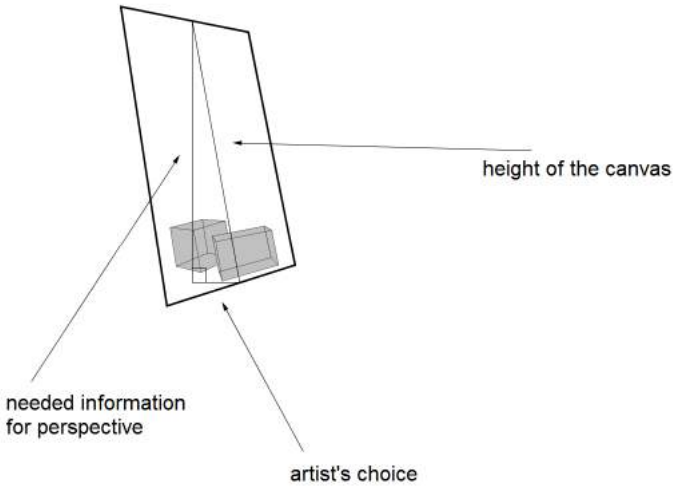

Figure 10: Canvas' inclination.

There are aspects of this interpretation that are pretty speculative. There are other aspects that are very likely: the matching with rigorous perspective and the Four thirds rule are mathematical facts. We do not know how truthful our interpretation is, but its internal logic consistency made it worth pursuing.

References

[1] Barker, C. "Allegory of Geometry by Laurent de la Hyre", *The Liberal Education Reporter*, 2011.

[2] Dussieux, L. et al. *Mémoires inédits sur la vie et les ouvrages des membres de l'Académie Royale de Peinture et de Sculpture*, Vol. I, 107, Paris, 1854.

[3] Heath, L. *The Thirteen Books of Euclid's Elements*, Dover Publications, 1956.

[4] Herodotus. *Histories*, Book II (Euterpe), 450 BC.

[5] Mariette, P., J. *Abecedario de P.J. Mariette et d'autres notes inédites de cet amateur sur les arts et les artistes*, Ouvmarage publié d'après les manuscrits autographes conservé au Cabinet des Estampes de la Bibliothèque Impériale et annoté par Ch(arles) Ph(ilippe) de Chennevières et A(natole) de Montaiglon, Archives de l'Art Français, Vol. IV, 48–49, Paris, 1854–1856.

[6] Sothebys: `www.sothebys.com/en/auctions/ecatalogue/lot.114.html/2014/the-courts-of-europe-n09107`

[7] Storey, G., A. *Theory and Practice of Perspective*, Dover Publications, 2006.

[8] Williams, E. Discussion of the copy of the Allegory of Geometry (Toledo Museum of Art), *Gods & Heroes: Baroque Images of Antiquity*, exhibition catalogue, 42–43, Wildenstein, New York, 1968.

[9] Wine, H., Ackroyd, P., Burnstock, A. "Laurent de La Hyre's Allegorical Figure of Grammar", *National Gallery Technical Bulletin*, Vol. XIV, 1993.

Appendix 1

Recreational Mathematics Magazine, Number 5, pp. 33–45
DOI 10.1515/rmm–2016–0003

Appendix 2

Recreational Mathematics Magazine, Number 5, pp. 33–45
DOI 10.1515/rmm–2016–0003

Games and Puzzles

Star tangrams

Robert Bates Graber, Stephen Pollard, Ronald C. Read
Truman State University, Truman State University, University of Waterloo
rgraber@truman.edu, spollard@truman.edu, ron.marie@cogeco.ca

Abstract: *The Tangram is a puzzle in which seven tiles are arranged to make various shapes. Four families of tangram shapes have been mathematically defined and their members enumerated. This paper defines a fifth family, enumerates its members, explains its taxonomic relationship with the previously-defined families, and provides some interesting examples.*

Keywords: Tangrams, combinatorics, spatial puzzles.

Introduction

In the puzzle known as the Tangram, players rearrange the seven tiles shown in Figure 1 to make various shapes.

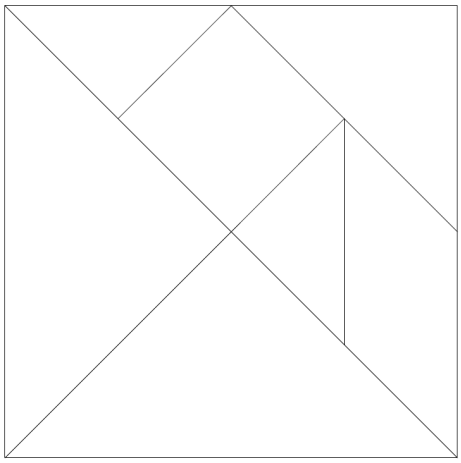

Figure 1: Tangram.

Some shapes are more or less representational; others are simply geometric forms. Shapes are often posed as "problems" — that is, as mere silhouettes or

outlines to be matched by the player's arrangement of the tiles. Problems commonly require that all seven tiles be used and that no subset of tiles be spatially separated from the others. Though the Tangram can be played competitively to see who can solve a given problem first, it is often played alone simply for aesthetic pleasure. The Tangram's modern form, which has been traced back to the early 19th century, evidently derives from designs for elaborate Chinese banquet-table suites and may have roots as deep as Liu Hui's 4th-century proof of the Pythagorean theorem. Devotees of the Tangram have included Lewis Carroll, Edgar Allen Poe, Napoleon Bonaparte, and John Quincy Adams [2].

Four families of tangram shapes (or problems) have been mathematically defined and the members of each have been enumerated [1, 3]. The purposes of this paper are to define a fifth type, to count its members, to explain its taxonomic relationship with the previously-defined types, and to provide some interesting examples.

Counting the Stars

A star tangram is simply one in which all seven tiles meet at a point (see Figure 2). In constructing such a tangram, it is natural to think of the tiles as converging at the central point; in appreciating the result as a star, however, it is more natural to think of them as radiating out from it. Because one of the tiles is a square, it will take up 90 degrees of the center; the remaining 270 degrees must accommodate the remaining six tiles. Since no tile has an interior angle less than 45 degrees, we have no way to compensate for an angle greater than 45 degrees. So each of the remaining six tiles must contribute a 45-degree angle to the central array. Note that each tile affords two orientations for touching the central point in this manner. For the five triangles, the second orientation can be found by either rotating or flipping the tile; for the parallelogram, flipping is necessary.

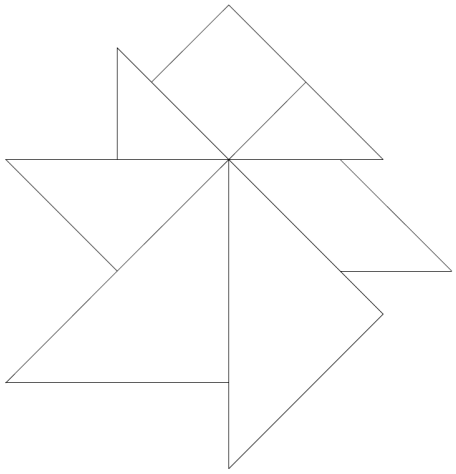

Figure 2: Star tangram.

To determine how many star tangrams are possible (the "star-tangram number") it is convenient to begin by considering only the arrangement of the tiles without regard to their orientations. Following [1], we label each of the two large triangles L; the medium one M; each of the two small ones S; the square Q; and the parallelogram Z. Adopting Q as our reference tile, we can think of the remaining tiles as candidates for the six positions shown in Figure 3.

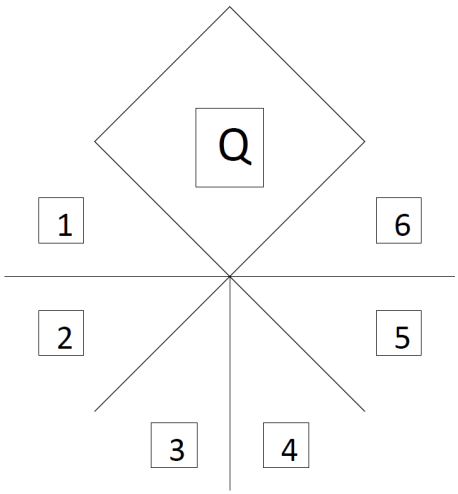

Figure 3: Six positions.

The number of possible arrangements may be thought of as the number of six-letter "words" that can be formed using L, L, S, S, M, and Z. Begin (arbitrarily) with the L's. They may occupy any two of the six positions. Their placement will leave only four positions for the two S's. *Their* placement will leave M a choice between two positions and Z must settle for the spot M leaves empty. The total number of possible arrangements, then, is:

$$\binom{6}{2}\binom{4}{2}\binom{2}{1}\binom{1}{1} = 180.$$

To denote the orientations of the tiles, it is helpful to consider Figure 2 in light of Figure 3. Note that in Figure 2 , as we move counterclockwise through the six positions, the leading abutting edge of each tile is always shorter than the trailing abutting edge. Taking capitalization to denote this kind of orientation and lower case to denote the reverse, we can specify Figure 2 's star, with regard both to arrangement of the tiles and to their orientations, by the designation SMLLZS. Reversing the orientation of the second tile would give us a new star designated SmLLZS.

How many such designations are possible? Because each of the six tiles can be placed, independently of the others, in either of two orientations, we must multiply the number of possible arrangements (180) by 2^6, this product being 11,520. It is conventional, however, to consider a tangram and its mirror image to be a single tangram. From this point of view, each of our designations has a

"looking-glass self" that we should not have counted. This is easily corrected: we simply divide by two, arriving at 5,760. (The correction would be a bit more complicated were it not that star tangrams, due to the odd couple M and Z, cannot be bilaterally symmetric.) It is also conventional to treat tangrams as the same when one is the result of rotating the other. This demands no correction from us, however, because our "word count" technique already ignores rotations. The designation SMLLZS says nothing about where, say, the square Q is sitting — even though, in Figure 2, we happened to place it at the top.

The Same Star?

But there is still a comparability problem. Previously-published numbers also consider any two tangrams having the same outline (or silhouette) to be a single tangram, regardless of their internal construction. Is it possible for a star's outline to remain the same despite a change in its internal construction? It is indeed, due to the square tile Q's interchangeability with the two small triangles (S and S) when the latter abut fully along their hypotenuses. (There are a few other promising-looking interchangeabilities, but they fail in one way or another to preserve star-ness.) This means we have, in effect, included some pairs of "twin" outlines, counting two where we should (for present purposes) have counted only one. To figure out how often this has occurred, it is helpful to return to Figure 3 and begin by considering how many places our two-piece square (SS) might occupy. Clearly, it can occupy positions 1 and 2, 2 and 3, 3 and 4, 4 and 5, or 5 and 6. Once it is in any one of these five pairs of adjacent positions, we will have four remaining positions for L and L, then two for M, and, finally, only one for Z. The number of arrangements, then, is:

$$\binom{5}{1}\binom{4}{2}\binom{2}{1}\binom{1}{1} = 60.$$

Now, the orientations of SS are fixed, but those of the other four tiles are free to vary; accordingly, we multiply by 2^4 to get 960. As before, we must divide by two to correct for mirror images. The 480 remaining tangrams, however, comprise 240 pairs of outline-twins differing only in that one has tiles Q and SS where the other has tiles SS and Q. (Figure 10, below, shows one member of such a pair.) Counting each pair as a single tangram, then, we must deduct 240 from 5,760. So the star-tangram number turns out to be 5,520.

A Catalog of Stars

Can we be sure that this figure is correct — that we have not, for example, overlooked some other way in which a star tangram can be produced more than once? There is a way to find out. In Figure 3, the Q piece is already inserted. Let A denote the collection of star tangrams obtained by inserting the other pieces into Figure 3 in all possible ways. As we have already seen, there are 180 ways of allocating the pieces to the six sectors and 64 ways of orienting those pieces within the sectors. Hence A will contain $180 \times 64 = 11,520$ tangrams.

One thing that is certain is that A will contain every possible star tangram at least once. To find how many of these are different we program a computer

to produce all the tangrams in A and output them as a file of 11,520 records, each record being a string of symbols giving the directions and lengths of the segments of the tangram's outline as we go round it in clockwise order. (This is somewhat similar to what was done in [1] to produce snug tangrams, but a bit more complicated since there are more possibilities for the lengths of the segments.)

We pass this file to another program which converts each record to a standard form ("standard" in the sense that tangrams that are equivalent under rotation or reflection will have identical standard forms, and conversely). In the final step, the program eliminates duplicate records, leaving just one record for each distinct tangram. All this was done, and the final list turned out to contain exactly 5,520 tangrams! This not only confirms the theoretical result but gives us an added bonus. From each record in the final output we can produce, electronically, a picture of the corresponding tangram. This has been done and there is now extant a "Picture Gallery" of all the star tangrams. (The first 480 entries of this gallery appear below in the Appendix.)

Other Families

How do these results relate to the four tangram numbers previously determined? Earliest — and by far smallest — is the convex-tangram number, famously proven in 1942 to be only 13 [3]. Convex tangrams, one of which is shown in Figure 1, have outlines free of indentations. None of the 13 is a star.

The convex tangrams compose a very small subset indeed of what more recently have been termed snug tangrams, the snug-tangram number having been determined, with computer assistance, to be 4,842,205 [1]. A snug tangram is defined as follows. Suppose the square Q has sides of length 1. Then the hypotenuse of a small triangle S has length $\sqrt{2}$. Indeed, each side of each tile consists either of a single segment of length 1, a single segment of length $\sqrt{2}$, two segments of length 1, or two segments of length $\sqrt{2}$. Snug tangrams obey the rule that when segments are in contact, they are in contact along their whole lengths with endpoints touching endpoints (a condition not all stars satisfy). Snug tangrams must also be free of internal voids (a condition all stars do satisfy).

The 45-degree angles in tiles L, M, S, and Z are all formed by an edge whose length is an integer (1 or 2) and an edge whose length is a multiple of $\sqrt{2}$ ($\sqrt{2}$ or $2\sqrt{2}$). This means that snugness will significantly constrain the placement of tiles in Figure 3. The tile that fills position 1 must have a trailing edge of integer length (since Q has sides of length 1) and a leading edge whose length is a multiple of $\sqrt{2}$. But then the next tile must have a trailing edge whose length is a multiple of $\sqrt{2}$ and a leading edge of integer length. And on it goes, from one position to the next, with the orientation of each new tile determined by that of the preceding one. The result is that very few stars are snug — only 81, or about 1.5 percent. (We leave the proof to the readers. For two examples, see Figures 6 and 8.)

A "bay" is an internal void that meets the perimeter of its host tangram at a

single point. A bay tangram has a bay but, otherwise, satisfies the definition of snugness (as in Figure 4). There are 731,951 bay tangrams [1]. A "hole" is an internal void that meets the perimeter of its host tangram at no point. A hole tangram has a hole but, otherwise, satisfies the definition of snugness (as in Figure 5). Their number is 9,360 [1]. Stars accommodate neither bays nor holes.

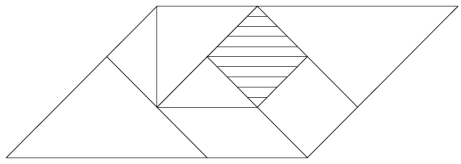

Figure 4: Bay.

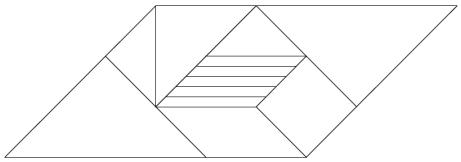

Figure 5: Hole.

Though there are over four hundred star tangrams for every one convex tangram, stars are rare compared with the other three types. For every star tangram, there are 877 snug tangrams and more than 130 bay tangrams (which seems quite remarkable); even the hole tangrams outnumber stars by a factor of nearly 1.7

Some Examples

Though star tangrams tend to have complex outlines and therefore tend to be relatively easy as problems, there are exceptions (e.g., Figures 6, 7, 8); and certainly the novel shapes they can take include many that are interesting, attractive, and suggestive (e.g., Figures 9, 10, 11, 12).

The examples in the Appendix offer a hint of the rich diversity of star-tangram shapes. They also present some amusing challenges for puzzlers — including various forms of wildlife and even Guinan from *Star Trek*. Can you find them?

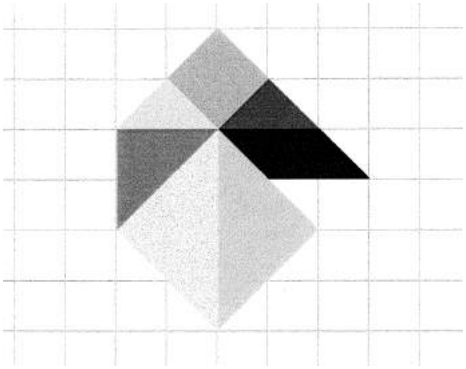

Figure 6: Example 1.

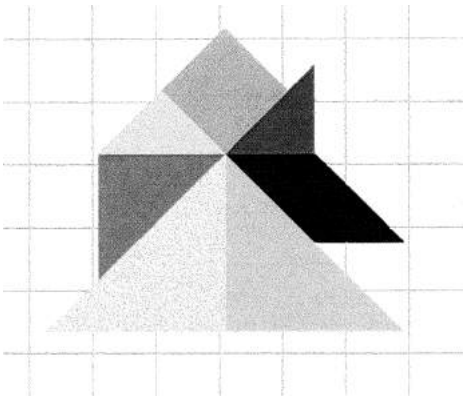

Figure 7: Example 2.

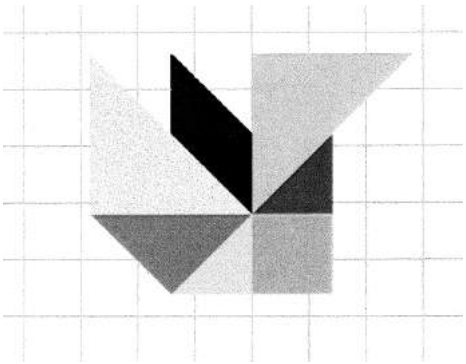

Figure 8: Example 3.

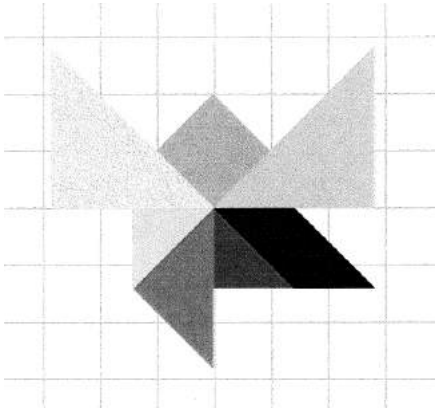

Figure 9: Example 4.

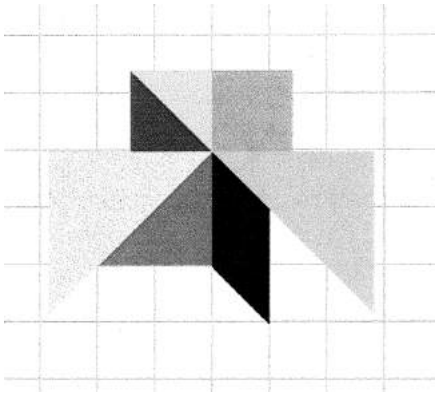

Figure 10: Example 5.

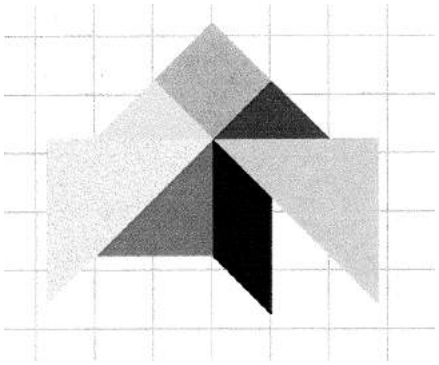

Figure 11: Example 6.

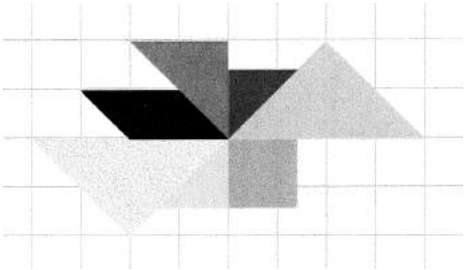

Figure 12: Example 7.

Acknowledgements

We are grateful to Jerry Slocum for encouragement and advice. Thanks, too, to Florence Emily Pollard for helping to make this paper more readable.

References

[1] R. C. Read. "The Snug Tangram and Some Other Contributions to the Corpus of Mathematical Trivia", *Bulletin of the ICA*, 40, 2004.

[2] J. Slocum, J. Botermans, D. Gebhardt, M. Ma, X. Ma, H. Raizer, D. Sonneveld, and C. Splunteren. *The Tangram Book*, New York: Sterling, 2004.

[3] F. T. Wang and C. C. Hsiung. "A Theorem on the Tangram", *American Mathematical Monthly*, 49, 1942.

Appendix

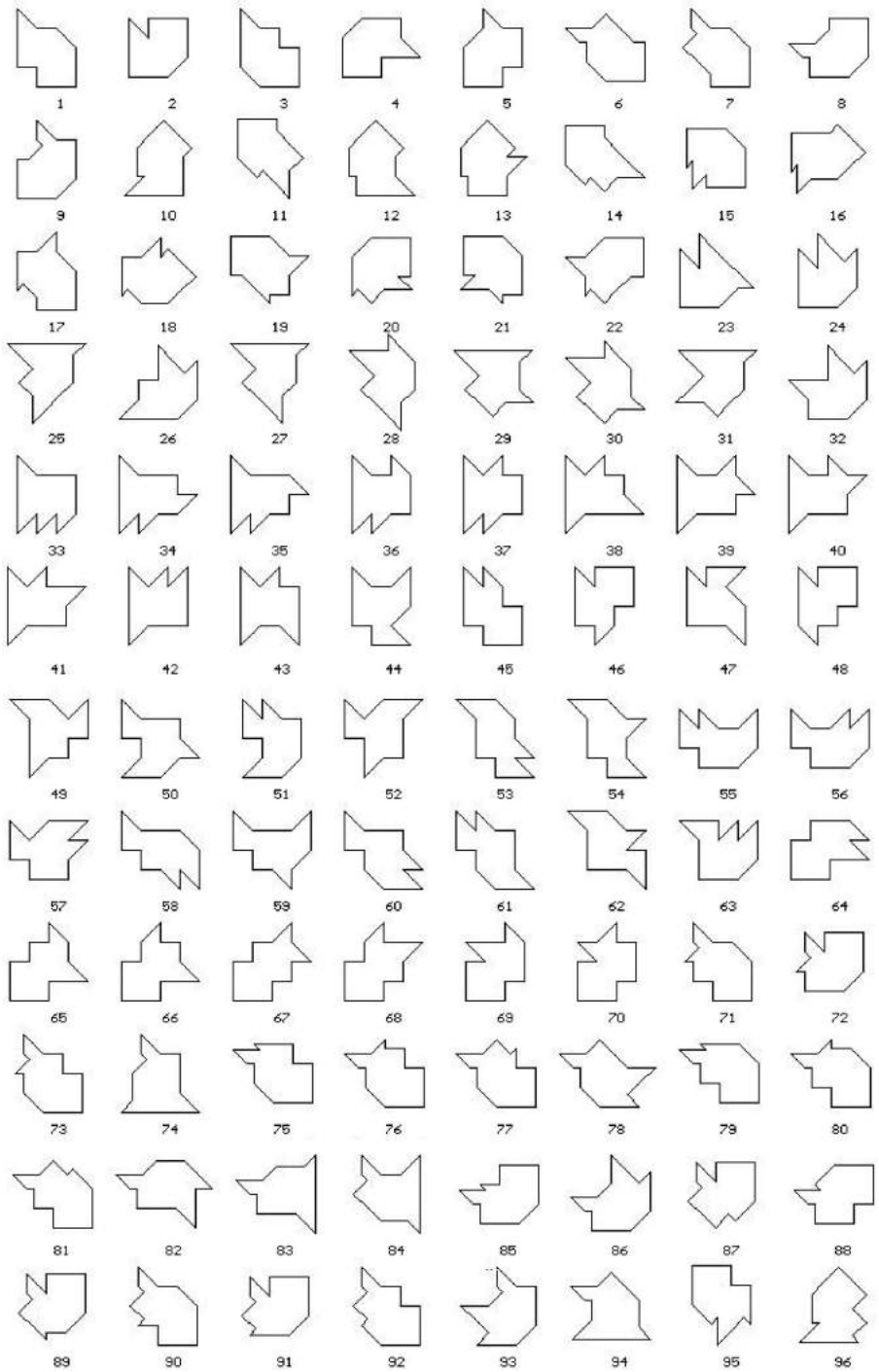

Recreational Mathematics Magazine, Number 5, pp. 47–60
DOI 10.1515/rmm–2016–0004

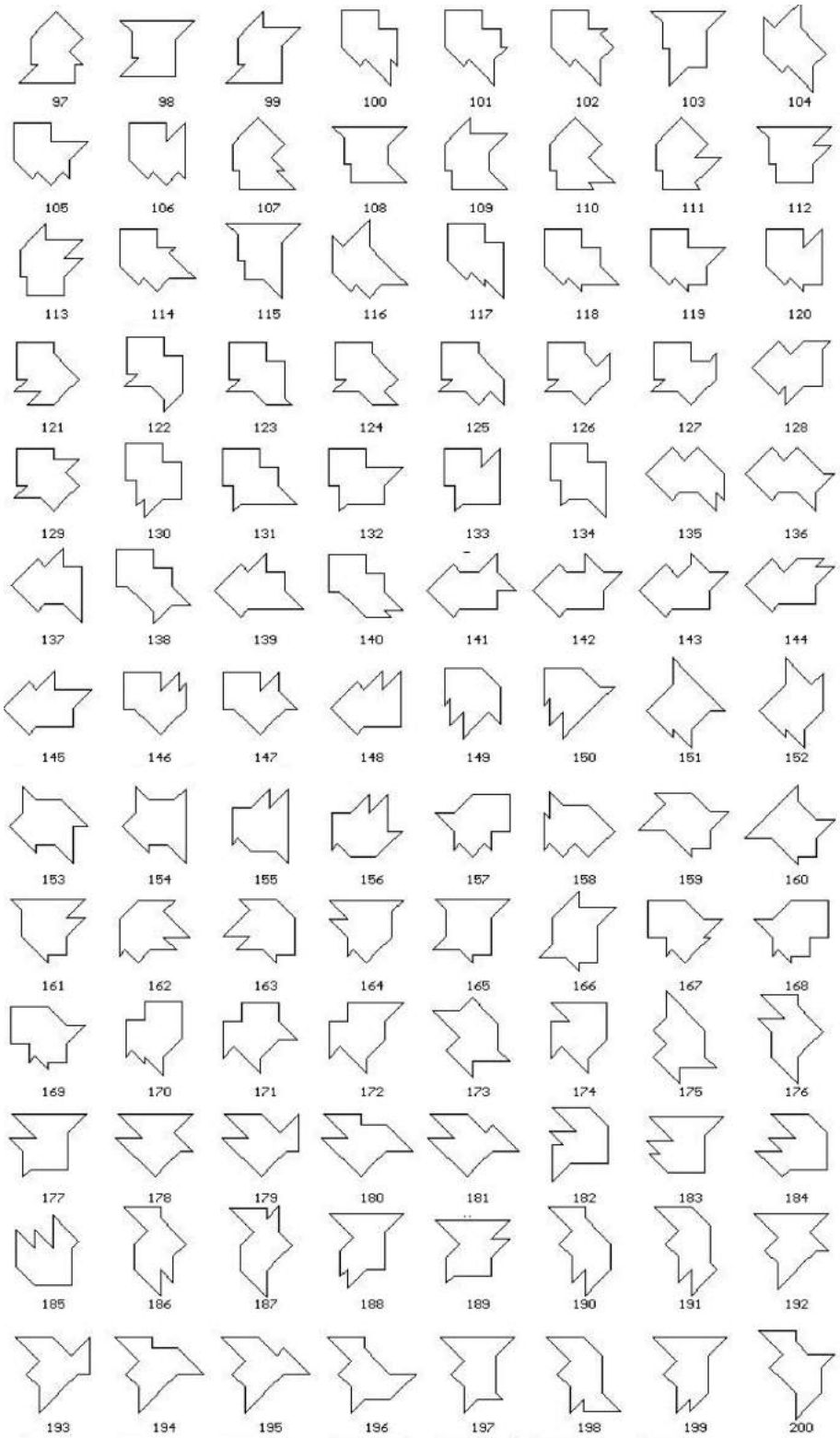

Recreational Mathematics Magazine, Number 5, pp. 47–60
DOI 10.1515/rmm–2016–0004

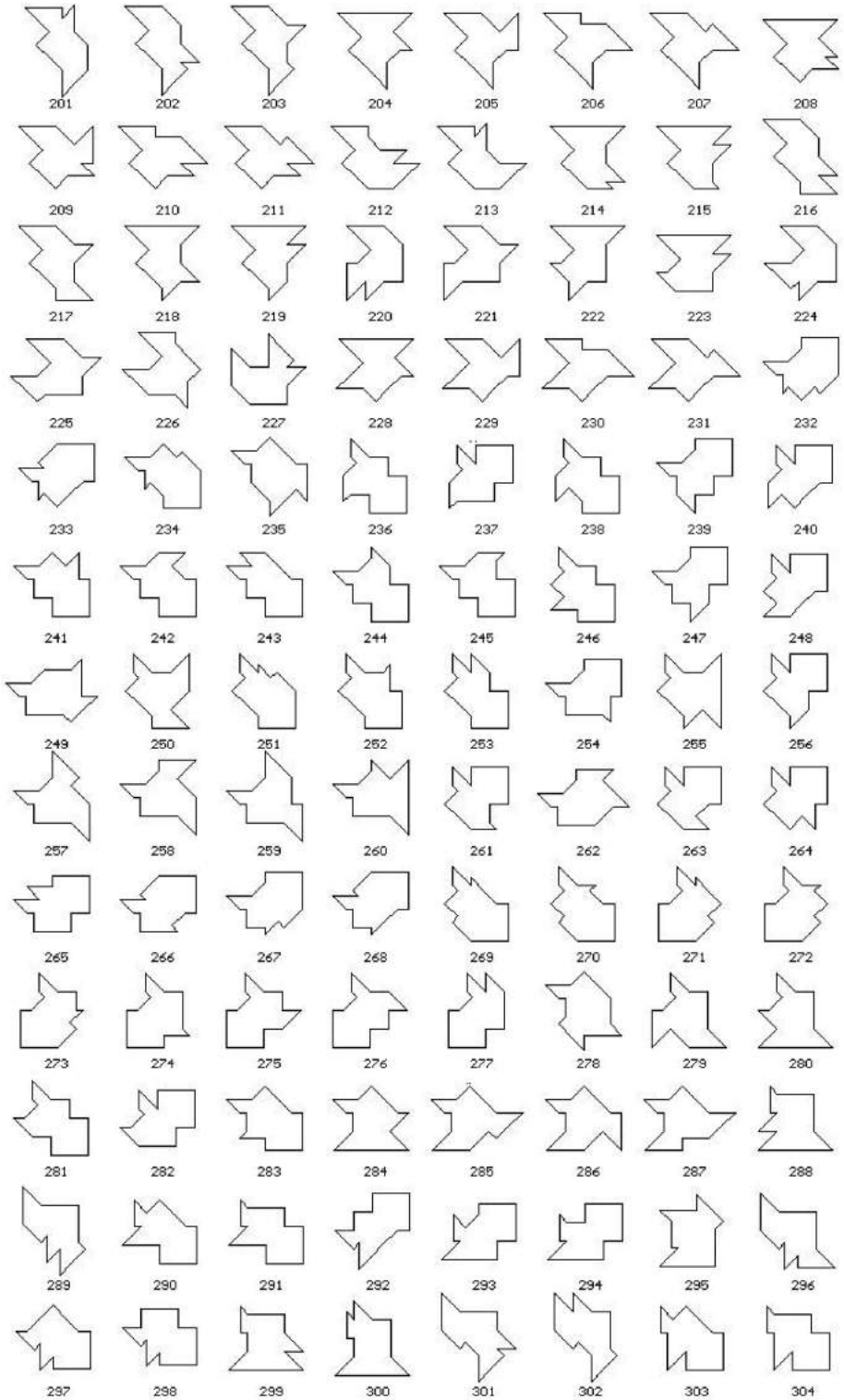

Recreational Mathematics Magazine, Number 5, pp. 47–60
DOI 10.1515/rmm–2016–0004

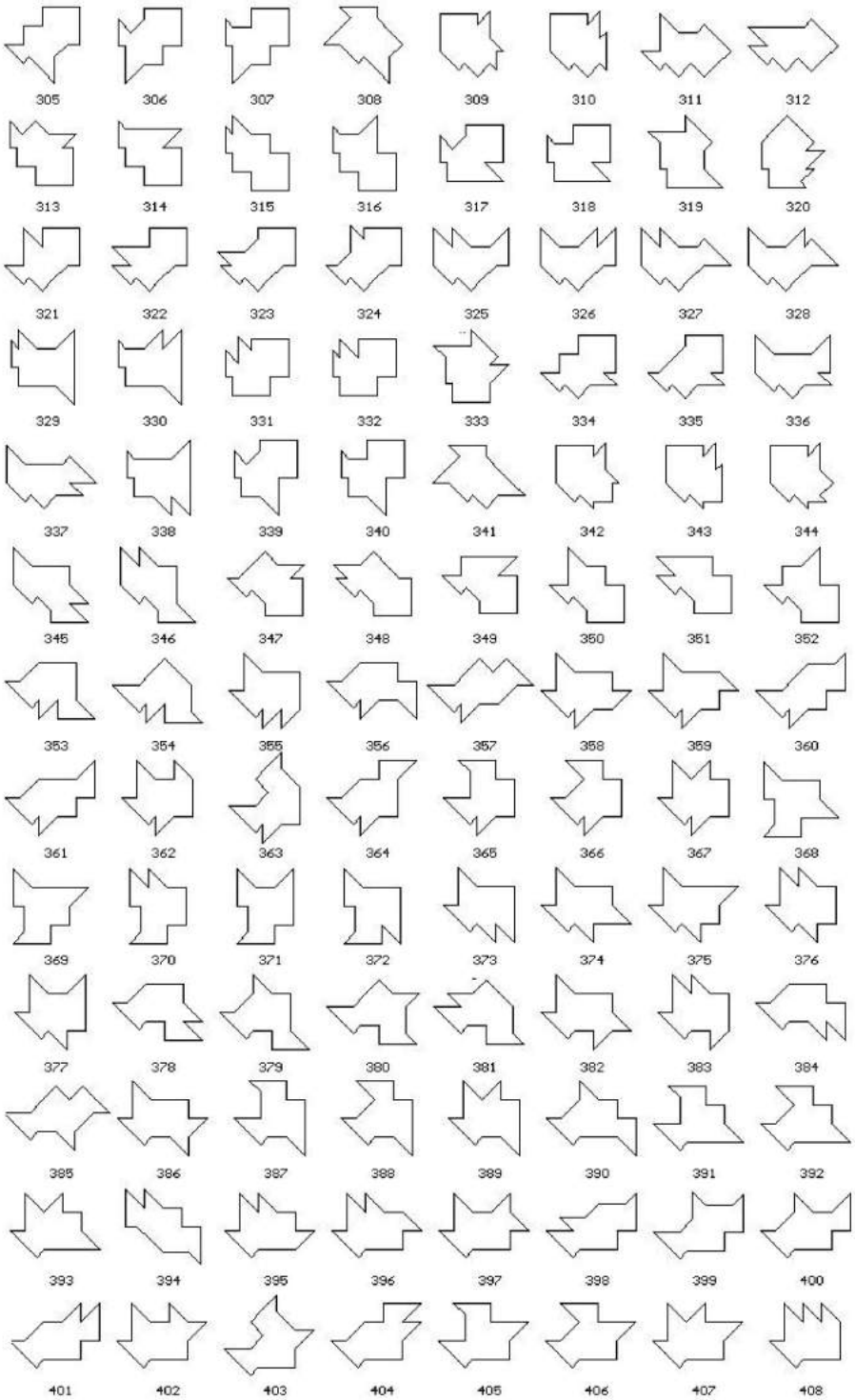

Recreational Mathematics Magazine, Number 5, pp. 47–60
DOI 10.1515/rmm–2016–0004

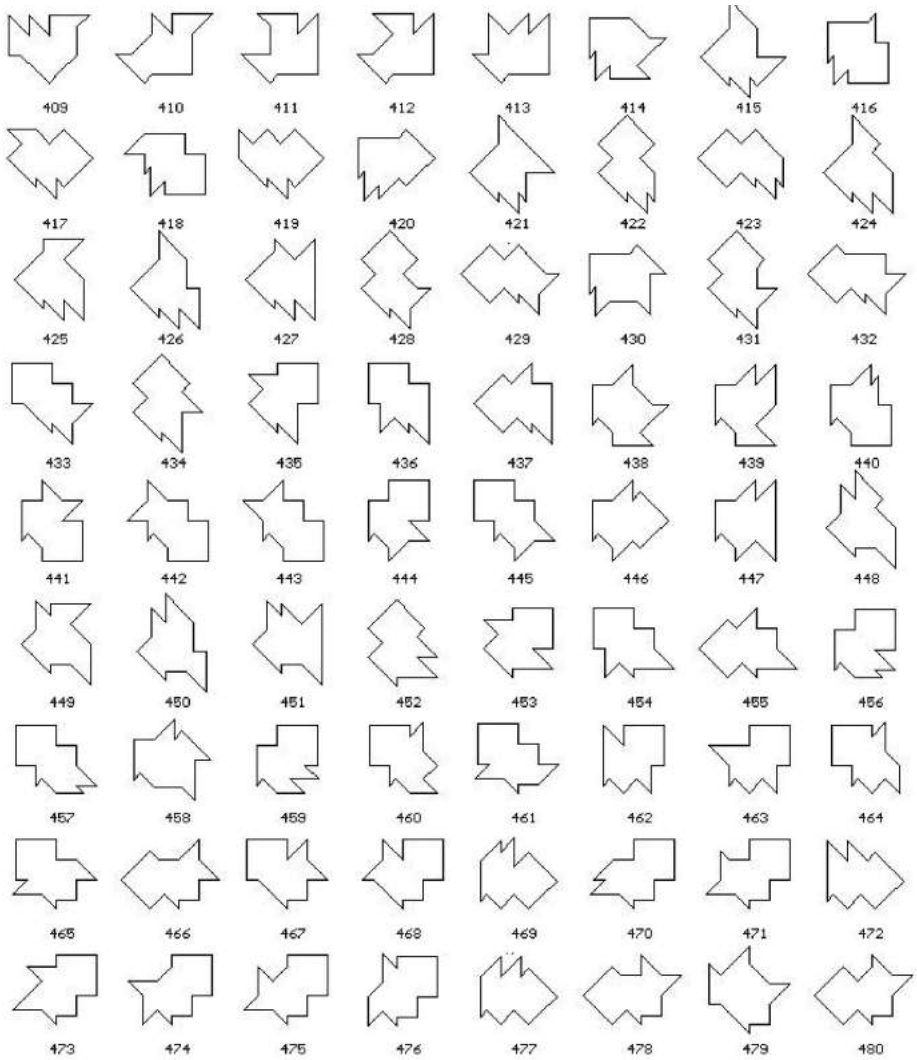

Recreational Mathematics Magazine, Number 5, pp. 47–60
DOI 10.1515/rmm–2016–0004

Games and Puzzles

Endless love: On the termination of a playground number game

Iain G. Johnston
School of Biosciences, University of Birmingham, UK
i.johnston.1@bham.ac.uk

Abstract: *A simple and popular childhood game,* LOVES *or the* LOVE CALCULATOR*, involves an iterated rule applied to a string of digits and gives rise to surprisingly rich behaviour. Traditionally, players' names are used to set the initial conditions for an instance of the game: its behaviour for an exhaustive set of pairings of popular UK childrens' names, and for more general initial conditions, is examined. Convergence to a fixed outcome (the desired result) is not guaranteed, even for some plausible first name pairings. No pairs of top-50 common first names exhibit non-convergence, suggesting that it is rare in the playground; however, including surnames makes non-convergence more likely due to higher letter counts (for example, "Reese Witherspoon* LOVES *Calvin Harris"). Different game keywords (including from different languages) are also considered. An estimate for non-convergence propensity is derived: if the sum m of digits in a string of length w obeys $m > 18/(3/2)^{w-4}$, convergence is less likely. Pairs of top UK names with pairs of 'O's and several 'L's (for example, Chloe and Joseph, or Brooke and Scarlett) often attain high scores. When considering individual names playing with a range of partners, those with no* LOVES *letters score lowest, and names with intermediate (not simply the highest) letter counts often perform best, with Connor and Evie averaging the highest scores when played with other UK top names.*

Keywords: Number games, name statistics, dynamic integer sequences, mathematics in schools.

Introduction

The LOVES game, variously known as the LOVE CALCULATOR, CRUSH COMPATIBILITY TEST and others, is played in various guises in playgrounds and classrooms across the world [4, 5]. The game has given rise to websites and apps peppering the web (for example, `http://www.lovecalculator.com`); and its whimsical nature has been cited as motivation in developing more rigorous game-theoretical approaches to assess compatibility [1]. LOVES is a word-and-

number game which attempts to assign a two-digit number to two character strings, by applying an iterated rule to a initial set of numbers, derived from the occurrence counts of certain letters within the strings. This note aims to explore the outcomes of this iterated rule for different real-world and general initial conditions, and for different game structures.

The game

We begin with two names. Occurrence counts of each letter in the word LOVES in the two names are recorded, and are expressed as a string of integers, which we will call $s^{(0)}$. For example, if Alice were playing with Bob, we would count 1 'L', 1 'O', 0 'V's, 1 'E' and 0 'S's, so $s^{(0)} = \{1, 1, 0, 1, 0\}$ (Figure 1).

We then move through the digits in the string from left to right. In this order, we sum each digit with the neighbour on its right, and append the sum to the rightmost position of new string $s^{(1)}$ (which starts off empty). So for Alice and Bob, the first pair of digits in $s^{(0)}$ (1 and 1) sum to 2, the next pair (1 and 0) sum to 1, the next to 1, and the final pair also to 1, so we arrive at the new string $s^{(1)} = \{2, 1, 1, 1\}$ (Figure 1).

When we reach the end of our previous string, we repeat this process for the new string that has been formed, leading to another new string. This process is iterated until we reach a string containing fewer than three digits. Following this process, we see $s^{(2)} = \{2, 1, 1, 1\} \to s^{(3)} = \{3, 2, 2\} \to s^{(4)} = \{5, 4\}$, whereupon the iteration terminates, having produced a string of length < 3 (Figure 1). The traditional conclusion of the game is to represent the two subjects' love as a percentage made from the final string: 'Alice loves Bob 54%!'.

More generally, given an initial string of digits $s^{(0)}$, the game consists of applying an iterative rule to the current string $s^{(t)}$ to produce a new string $s^{(t+1)}$:

$$s^{(t+1)} = (s_1^{(t)} + s_2^{(t)}) \,||\, (s_2^{(t)} + s_3^{(t)}) \,||\, ... \,||\, (s_{n_t-1}^{(t)} + s_{n_t}^{(t)}), \tag{1}$$

where s_i denotes the ith digit in string s, n_t is the number of digits in string $s^{(t)}$, and $||$ is the concatenation operator.

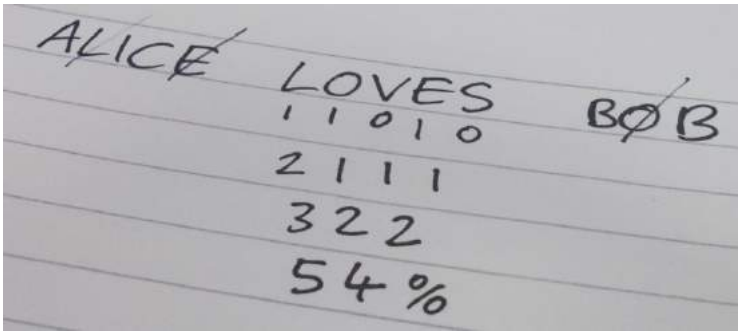

Figure 1: The LOVES game played by Alice and Bob, as described in the text.

Several variations exist, including changes to which letters or sets of letters are counted. Sometimes an additional modular number game, FLAMES, is played to decide the mode of interaction: (Friendship, Love, and others).

Results I: Types of love

General behaviour

We observe three types of behaviour produced by different initial strings: *termination*, *looping*, and *divergence*. Termination is illustrated by the example above and in Figure 1: a string of length < 3 is reached after some finite number of iterations. The other two 'endless love' cases never reach this target. Looping involves a periodic cycling between two or more different strings of length $\geqslant 3$, repeated forever. Divergence involves an unbound increase in string length as iterations continue. Table 1 contains examples of these different behaviours.

Termination	$\{1,1,0,1,0\} \to \{2,1,1,1\} \to \{3,2,2\} \to \{5,4\}$
Looping	$\{1,4,1,2,1\} \to \{5,5,3,3\} \to \{1,0,8,6\} \to \{1,8,1,4\} \to \{9,9,5\} \to \{1,8,1,4\} \to ...$
Divergence	$\{6,6,6,6,6\} \to \{1,2,1,2,1,2,1,2\} \to \{3,3,3,3,3,3,3\} \to \{6,6,6,6,6,6\} \to \{1,2,1,2,1,2,1,2,1,2\} \to ...$

Table 1: Examples of the three types of outcome of the game.

Two looping 'motifs' can be identified, namely a period-2 cycle $\{9,9,...\} \to \{1,8,1,...\}$ and a period-3 cycle $\{3,3,3,3,...\} \to \{6,6,6,...\} \to \{1,2,1,2,1,...\}$, where the ellipses in the first step given refer to at least one other digit. Depending on the subsequent digits, these motifs may also form part of divergent strings (and usually do if there is more than one other digit; hence, these motifs will usually not give rise to looping behaviour if included as part of an initial length-5 string).

Distribution of outcomes by starting set

We first investigate the distribution of behaviours across different sets of initial strings. We will restrict our analysis[1] to starting strings where all letter counts are under 10. Initially, we consider sets of strings classified by an integer label c. A set with label c contains all strings of five integers which all have values less than c. Hence, $c = 10$ corresponds to the set $\{0,0,0,0,0\}...\{9,9,9,9,9\}$ of all five-digit strings; $c = 2$ corresponds to the set $\{0,0,0,0,0\}...\{1,1,1,1,1\}$ of all binary strings of length five.

Figure 2 shows the distribution of game outcomes over sets with $c = 4, 6, 8, 10$. We can see that the proportion of divergent strings increases towards 1 as c increases, suggesting that initial strings containing higher digits are more likely to diverge. Looping behaviour is rather more rare: the proportion of looping strings is under 0.03 for $c = 4$ and decreases as c increases. The proportion of terminating strings decreases with c in concert with the increasing likelihood of divergence. Of those strings that do terminate, the pattern of final outcomes displays complicated structure, which is to some extent conserved across different c values. Multiples of 10 are notably rarer than other outcomes, as only one

[1] The extension to initial counts over 10 will be seen to fall naturally into our analysis when we consider longer starting strings.

string can give rise to these final values: the outcome $10n$ is only produced by the string $\{n, 0, 0, 0, 0\}$. Regions of high occurrence occur across c values in the ranges $15-22$, $50-55$, $62-68$ and $85-92$, providing a rather mixed outcome for potential lovers: the reason for this structure currently remains elusive.

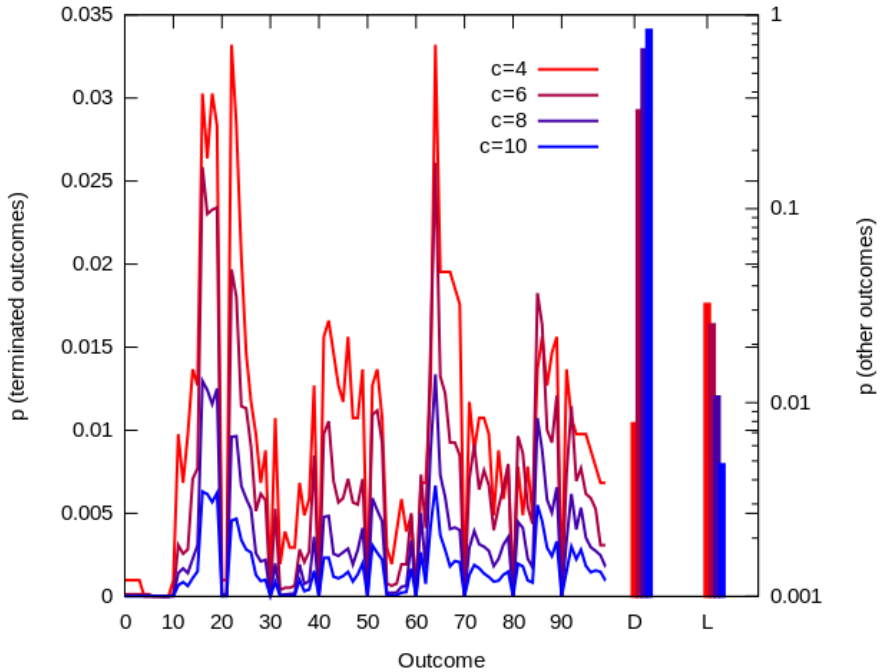

Figure 2: Frequencies of different outcomes of LOVES when played with all different starting strings consisting of five digits less than c. Left hand side (linear vertical axis) shows individual results (0%...99%) of terminating strings; right hand side (logarithmic vertical axis) shows 'endless love' cases: D – divergent; L – looping.

Distribution of outcomes by starting magnitude

Noting that divergence appears to be more common for strings containing higher digits, we assign a descriptor of a string, its *magnitude* m. For a string s of length L we define m simply as the sum of all digits in the string $m = \sum_{i=1}^{L} s_i$. The observations above suggest that divergence propensity will increase with m.

To explore the influence of magnitude on the probability of 'endless love', we subdivide the set $c = 10$ into strings labelled by m, and compared the outcome behaviour of each of these m-labelled subsets. Figure 3 shows these results: there is a monotonic increase of divergence probability with m, with divergence probability saturating at 1 as m increases. No strings with $m > 27$ terminated (the terminating $m = 27$ case is illustrated by $\{7, 3, 9, 1, 7\}$, which terminates at $\{6, 5\}$ after 24 iterations).

Terminating strings with high m tend to display motifs where several pairs of adjacent digits sum to 10. This property is clearly exhibited by the $m = 27$ example above; others include $\{5, 2, 8, 2, 9\}$ ($m = 26$, $\{8, 5\}$ after 17 iterations) and $\{1, 5, 5, 5, 9\}$ ($m = 25$, $\{2, 2\}$ after 27 iterations). Intuitively, these strings immediately expand into strings containing $\{..., 1, 0, 1, 0, ...\}$ which then collapse, diminishing string length and yielding small numbers in the next iteration: a hint to players who want to ensure their love remains bound. In the Appendix we analyse in more detail the length of the 'decay chains' by which an initial string evolves, and the behaviour of the string length as this process progresses.

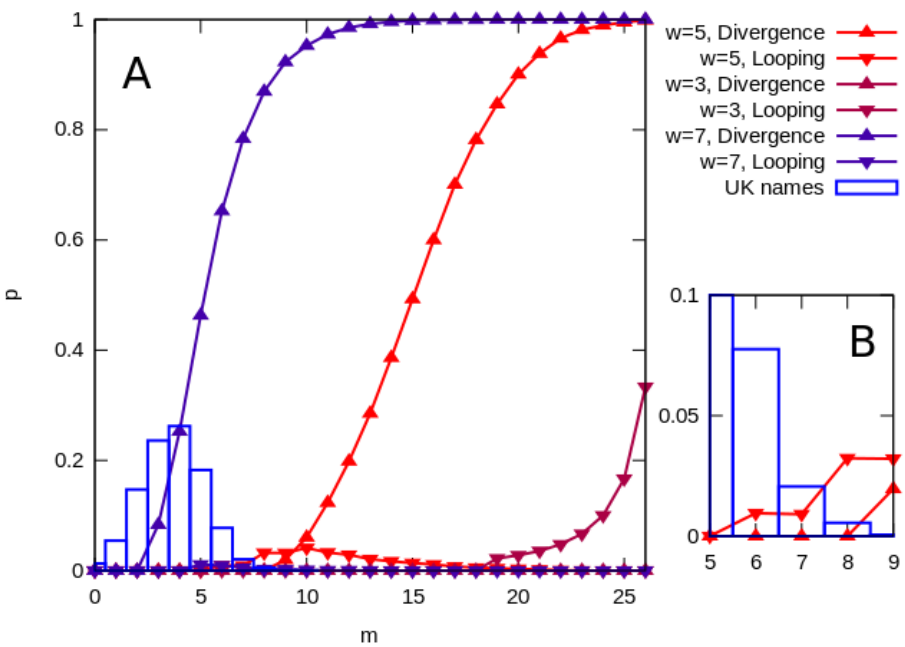

Figure 3: Outcomes of games over the set $c = 10$ as a function of start string magnitude m and length w (LOVES corresponds to $w = 5$; other games are discussed later in the text). (A) Probability that a string diverges or loops with m; histogram shows the distribution of magnitudes found when playing LOVES with random pairings of popular UK first names (see text). (B) Same plot with focus on the region where UK name distribution overlaps with a nonzero looping probability for $w = 5$.

Termination of combinations of real names

The non-terminating behaviour of the game may be surprising to readers who did not encounter this behaviour in the playground [2]. We next seek to explain this by considering the game behaviour with initial strings that are likely to

[2] Although the looping behaviour has been previously been observed by some players; for example, by commenters on this discussion `http://www.lawoftheplayground.com/browse.php?type=subject&id=2449`

appear in real games. To this end, we use lists of the 50 most popular baby boys' and girls' first names in the UK in 2010 [6] (thus presumably populating playgrounds today)[3]. The initial number strings arising from all boy-girl, boy-boy, and girl-girl pairings of these names were computed, and the magnitudes of these 'realistic' strings were compared to our findings in the previous section. There is indeed little overlap between the magnitudes arising from common UK name pairings and the magnitudes leading to non-termination (Figure 3 inset). Although a small amount of overlap with looping magnitudes did exist, no specific pairs of top-50 names exhibit this behaviour. It is straightforward to construct reasonable cases that do, however: consider 'Steve-O LOVES Esmie' $\rightarrow \{0,1,1,4,2\}$ $(m = 7)$, which collapses to the $\{9,9,1\} \leftrightarrow \{1,8,1,0\}$ loop. Including surnames in the game makes achieving the magnitudes required for non-convergence easier: for example 'Reese Witherspoon LOVES Calvin Harris' $\rightarrow \{1,2,1,4,3\}$ $(m = 11) \rightarrow \{9,9,6\} \leftrightarrow \{1,8,1,5\}$.

The distribution of outcomes from the set of common UK names is shown in Figure 4. There is substantially different structure compared to the full $c = 10$ set, even when the higher probability of termination is accounted for: the landscape of peaks of high occurrence is more rugged and does not obviously correlate with the common regions previously noted, with a (rather unfortunate) skew of terminating strings towards lower final results. One reason for this is the dramatic difference in letter frequencies among UK names compared to a uniform sampling: V in particular is highly underrepresented (Figure 4 inset). Generally lower numbers in the central position of the start string may be expected to give rise to differences in game outcome. Our exhaustive search of $c = 10$ led to the observation that for a count of zero 'V's, compensatory high counts for other characters (two counts of 4, or one of 3 and one of 5), are required to prevent termination; the requirement for a compensatory high count even for a single V is illustrated in our example above.

If we remove the infrequent V and replace it with commoner letters, we add a degree of nonsense to the literal interpretation of the game, but can discover looping behaviour among common UK names. For example, 'Connor LORES Harrison' $\rightarrow \{0,3,3,0,1\}$, which collapses to the $\{9,9,4\} \leftrightarrow \{1,8,1,3\}$ cycle.

Other games

We have seen that 'endless love' is a rare occurrence in UK playgrounds. How much is this an unfortunate result of linguistics? A natural extension of the LOVES game is to consider different central words: varying the length of the initial string of numbers will intuitively impact on the outcome of the game. Here we consider the case where the central word consists of w strictly different letters. Cases where the central word contains repeated letters (for example, ELSKER in Norwegian), and some elements in the initial number string are thus forced to be identical, constitutes a further extension to be explored in future.

As expected, we observe an increase in divergence propensity with increasing w, for the $c = 10$ set (where the set of initial strings is now understood to consist

[3]Readers may be interested that 'Olivia' and 'Oliver' occupy the female and male top spots; a selection of other names feature in Table 2.

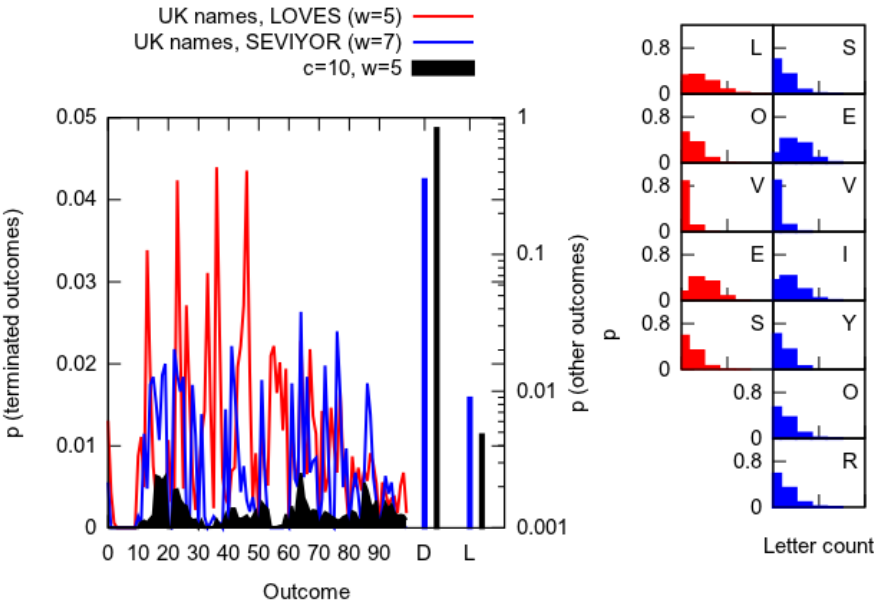

Figure 4: (left) Outcomes of the LOVES and SEVIYOR games with the set of common UK name pairings, compared to LOVES with the set $c = 10$ (as in Figure 2). D – divergent, L – looping. (right) Distributions of letter counts among the set of common UK pairings.

of all strings of length w consisting of numbers under c), illustrated in Figure 3. The sigmoidal relationship between magnitude and divergence frequency is shifted to lower m and sharpened as w increases, indicating that lower magnitudes can achieve non-convergence.

An interesting result of increasing w is the shift of divergent magnitudes into the range occupied by common UK name pairings. For example, if UK children were to play using the $w = 7$ Turkish word SEVIYOR, Figure 3 predicts that divergent behaviour would be much more common. This prediction is borne out by simulations pairing common UK names and playing SEVIYOR – the proportion of divergent name pairings rises from zero to around a third of all pairings (Figure 4), showing that 'endless love' may be rather more common in non-English-speaking playgrounds.

Results II: The path to love

Mean trajectories of strings

To understand how players may predict their propensity for 'endless' or bounded love, we now take a more analytic view of a given game. If we consider a chain as a 'walk' in (w, m) space, different pairs of adjacent numbers in the current string

can give rise to two different walking behaviours. For a single pair ($w = 2$), if the sum of the numbers < 10, the effect of that pair on application of Equation 1 is to leave m unchanged and reduce w by 1. If the sum of the numbers $\geqslant 10$, m is reduced by 9 and w remains the same.

A string can be viewed as a collection of $w - 1$ pairs, where each digit except the first and last contribute to two pairs. The extension of the above $w = 2$ picture is as follows. The maximum attainable magnitude in the next step is $m' = s_1 + s_w + 2\sum_{i=2}^{w-1} s_i$, and the maximum attainable length is $w' = 2(w-1)$. Each pair that sums to < 10 contributes $\Delta m = 0, \Delta w = -1$; each pair that sums to $\geqslant 10$ contributes $\Delta m = -9, \Delta w = 0$. It will readily be seen that the statistics of the string after an iteration of Equation 1 are $w \to w' + \Delta w, m \to m' + \Delta m$.

Hence, for $\{9, 9, 9, 9, 9\}$, we have $m' = 72, w' = 8$; all four pairs sum to > 10, so we have $\Delta m = -36, \Delta w = 0$, giving $m = 36, w = 8$, the statistics of $\{1, 8, 1, 8, 1, 8, 1, 8\}$. As another example, for $\{1, 0, 9, 2, 2\}$ we have $m' = 25, w' = 8$; three pairs sum to < 10 and one to > 10 so we have $\Delta m = -9, \Delta w = -3$, giving $m = 16, w = 5$, the statistics of $\{1, 9, 1, 1, 4\}$.

We write n for the number of pairs in a string that sum to $\geqslant 10$. The total number of pairs is $w-1$: hence, $w-1-n$ pairs sum to < 10. The next iteration is then characterised by

$$m \quad \to \quad m' - \Delta m = s_1 + s_w + 2\sum_{i=2}^{w-1} s_i - 9n \tag{2}$$

$$w \quad \to \quad w' - \Delta w = 2(w-1) - (w-1-n) = w - 1 + n. \tag{3}$$

We can begin to estimated the expected action of iterating Equation 1 by considering the dynamics that it provokes in (w, m) space. To proceed, we record the average $(\Delta w, \Delta m)$ resulting from an application of Equation 1 to all strings that occupy a given point in (w, m). This averaged quantity $(\langle \Delta w \rangle, \langle \Delta m \rangle)$ gives the expected movement in (w, m) space for each point.

Figure 5 plots the averaged step $(\langle \Delta w \rangle, \langle \Delta m \rangle)$, taken over all strings with a given (w, m). The structure of the expected step behaviour in the (w, m) plane immediately sheds light on the dynamics we have seen so far. Low (w, m) strings (Figure 5a) experience moderate increases in m in concert with decreases in w. For sufficiently low starting m, the small magnitude of m increase allows these dynamics to reach $w = 2$ without exceeding a 'critical line' of m. There is also a region of $w = 3$ strings with high m (Figure 5b) where an iteration produces an increase in w, but coupled with a sufficient loss of m to keep strings in the low-(w, m) region.

Outside this region, two behaviours are visible. For high w and low m (Figure 5c), decreases in w are induced by iteration, but accompanied by large increases in m. The trend to decreasing w suggests that $n = 0$ is common in this region (from Equation 3). For high m (Figure 5d), iterations induce decreases in m accompanied by often dramatic increases in w, suggesting (Equation 3) that $n > 0$ in this region. The action of these two trends is to force strings towards

a noticeable line of divergence around region (5e) and above, where iterations leads to increases in w with moderate increases in m, with no upper bound. The slow changes in w in this line of divergence suggests that $n \simeq 1$ in this region. This splitting of the phase portrait by n is indeed what is observed, as can be seen in the demarcated regions of $\langle n \rangle$ (n averaged over all strings for a given (w, m)) in Figure 5.

Figure 5 of course only represents an 'averaged' behaviour, but the agreement with the observed divergence propensities is striking. It can be seen that movement towards the $\langle n \rangle \simeq 1$ band in Figure 5 is a central determinant of eventual behaviour. As long as $n = 0$, w decreases; divergence requires steps with $n > 0$. For a given w, the value of m marking the transition from highly-likely termination to highly-likely divergence seems to correspond to the region where the averaged result of a step avoids the $\langle n \rangle \simeq 1$ band until $w \leqslant 4$.

For $n = 0$, Equation 2 gives bounds on the step in magnitudes that occur with the $w \to w - 1$ transition. In the Appendix, we show that a prediction for the transition line separating convergent from non-convergent regions of (w, m) space occurs approximately at

$$m^* \simeq \frac{18}{(3/2)^{w-4}} \tag{4}$$

which agrees with observations in Figure 5.

Termination result and magnitude

The anticipated question, what properties of an initial string predict termination at a high final 'love' outcome, remains challenging to answer. No simple properties of $w = 5$ strings, including m, individual s_i values, and linear combinations of s_i values, and differences between adjacent s_i, were found to correlate with either termination magnitude or the final result at termination (defined as $10s_1 + s_2$). Figure 5 hints at a possible strategy for maximising final m: choosing an initial point in (w, m) space that maximises m while avoiding the $n = 1$ zone. However, the nonlinearity in the iterative process, and the pronounced string-to-string variability in specific behaviours from any (w, m), makes even this approach unreliable; and further extension from final magnitude to final result is also difficult. Figure 6 shows the probability of different outcomes for different strings of magnitude m; while there is a slight trend for *terminating* strings of higher m to yield higher results than terminating strings of lower m, the decreasing number of terminating strings of high m diminishes this trend when all strings are considered.

Even explicitly 'backtracking' from a desired target string fails to yield much intuitive progress. In the Appendix we show that in the absence of length-expanding steps ($n = 0$ everywhere), the initial string giving a final result $\{s_1, s_2\}$ is

$$\{a_3, a_2 - a_3, a_1 - 2a_2 + a_3, s_1 - 3a_1 + 3a_2 - a_3, s_2 - 3s_1 + 6a_1 - 4a_2 + a_3\}\,, \tag{5}$$

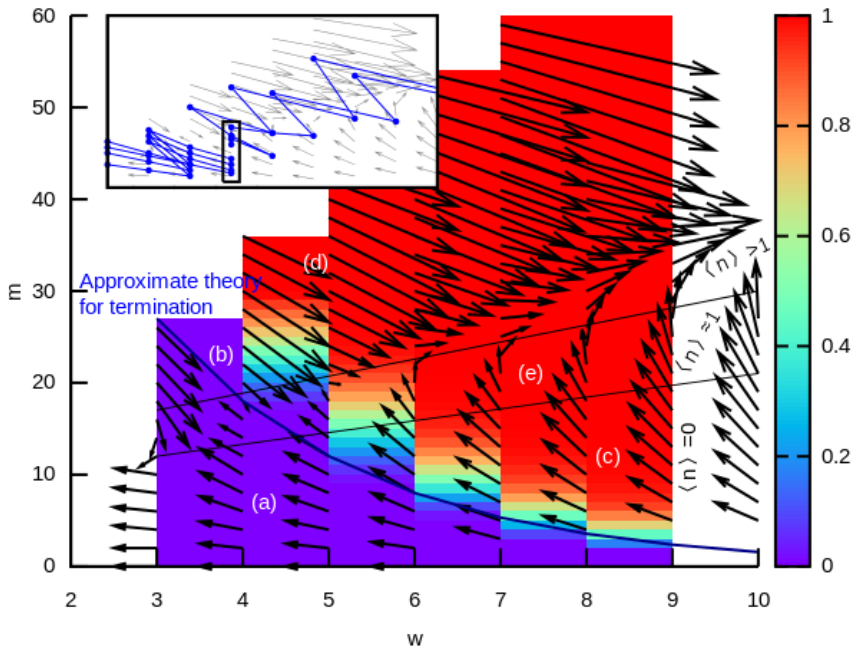

Figure 5: Mean trajectories in (w, m) space. Coloured background shows the probability of divergence for each (w, m) point. Black vectors show step magnitude and direction, upon one iteration of the game rule, averaged over all strings corresponding to a given (w, m). Black lines roughly divide (w, m) space by $\langle n \rangle$, the number of length-increasing transitions. The blue line gives a theoretical estimate for the boundary of the region of divergence from Equation 4. Inset shows some example trajectories from specific terminating (leftwards) and divergent (rightwards) strings, from different source strings within the black rectangle.

for a set of digits a_1, a_2, a_3 that can to some extent be specified. However, the numerous inequalities that a_1, a_2, a_3 must satisfy to yield a valid decay chain (see Appendix) prevent the straightforward choice of a starting string to give a desired result; integer programming, which is NP-hard, is required to make progress within this picture [3]. The question of what intuitive features, if any, predict whether a given starting string will terminate with a high final value remains open.

One step towards an answer is to examine the set of initial strings that give rise to high final results. Many strings yield 99%, from the $m = 3$ $\{0, 0, 3, 0, 0\}$ to the $m = 24$ $\{9, 1, 9, 3, 2\}$; of the 10^5 strings with $c = 10$, 97 give 99% and 731 give 95% or above. However, many of these would not plausibly arise from real names; restricting strings to $m < 10$ and the number of 'V's to be under 3 gives 76 strings giving 95% or above. Only 10 occur in combinations from the list of top-50 UK names (Table 2). Heuristically, names with pairs of 'O's or high counts of 'L's are among the top scores, though this is not a rigorous rule.

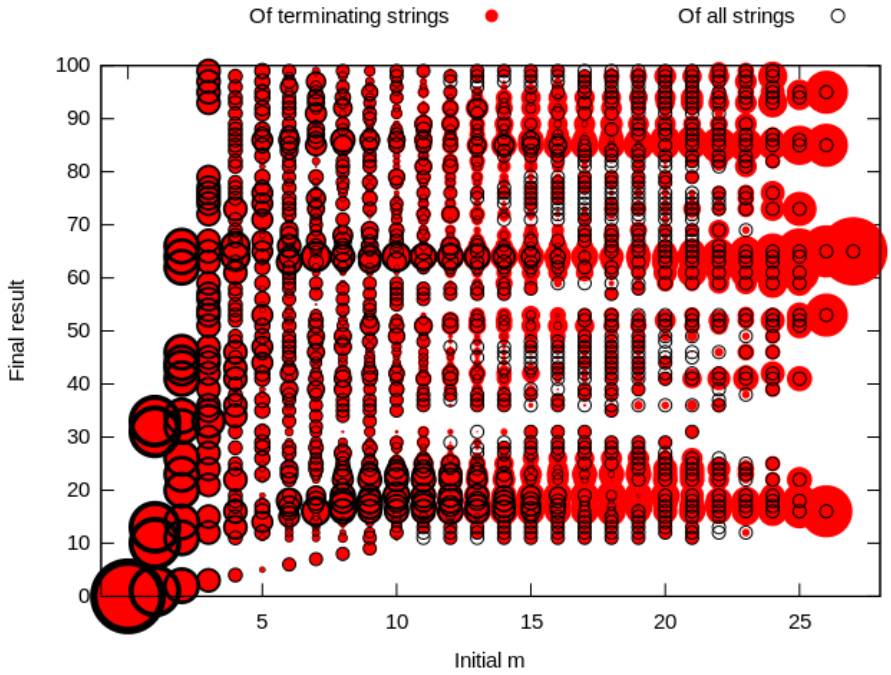

Figure 6: Probability of a given final result $10s_1 + s_2$ from a terminating string with initial magnitude m. Radii of filled circles are proportional to the log probability that a *terminating* string of magnitude m produces an output; radii of empty circles are proportional to the log probability that *any* string of magnitude m produces an output.

One can also consider the individual names that score best when the game is played with other names. Of course, the performance of individual names is identical if they contain the same counts of the LOVES letters. We therefore consider the sets in $c = 3$ (deemed realistic for real-world names) that have the highest average score when played with all 100 top UK names. Ranked by average score and omitting the string notation for brevity, the winners were 21012, 20110, 01102 and 00200, averaging 69.76% across the set of names. The winning sets that themselves correspond to top-50 names were 02000 (Connor), scoring 67.42% on average, and 00120 (Evie) scoring 66.69%. The bottom was the set 00000, scoring 25.75%, with corresponding names ranging from Adam to Ryan (and, sadly, the author's own name). One notable property of the set of high-scoring $c = 3$ sets is intermediate magnitudes: sets with $3 \leqslant m \leqslant 6$ score more highly on average when played with UK names than those with higher or lower m (Figure 7).

Ranked by number of $\geqslant 95\%$ scores, the winning set is 00222 (with 28 partners giving $\geqslant 95\%$), followed by 12010 and 21101, each with 26 partners. By this criterion, the highest-ranking sets with top-50 names were 02010 (Brooke) with 20 partners and 11100 (Olivia) with 16 partners; again, the 00000 set ranked lowest, tying with several others with 0 partners yielding $\geqslant 95\%$ scores.

Players with names matching the high-scoring strings given here and in Table

2 are more likely to score highly when playing LOVES with a randomly chosen partner. We note that 'Vivian', while not a top-50 UK name, seems set to experience romantic success, matching the top-scoring 00200 string.

High scoring ($\geqslant 95\%$) complete starting strings				
Names scoring 99%			Sets	Score
Joseph an d Leo, Chloe, Charlotte			02100, 22010	95
Brooke and Lewis, Samuel, Scarlett			10140, 22011	96
Sophie and Leo, Chloe, Charlotte			21110, 41020	97
			12020, 21111, 41021	98
			12021	99
Score averaged over game partners: Single names			**All $c = 3$ sets**	
Names	Average %	Set	Set	Average %
Adam Amy Hannah Harry Jack Max Mia Muhammad Nathan Ruby Ryan	25.75	00000	00000	25.75
Daisy Isaac	26.76	00001	00001	26.76
Abigail Dylan Liam Lucy	35.75	10000	00002	27.76
Isla Lucas	36.76	10001	22211	34.99
Archie Benjamin Edward Emma Erin Ethan Freya Grace Henry Jake Jamie Jayden Katie Matthew Megan	37.90	10001	22210	35.57
James Jasmine Maisie Sienna Summer	38.96	00011	01222	35.74
Jessica	40.00	00012	10000	35.75
Oliver	44.55	11110	12220	36.22
Callum Layla Lily William	44.85	20000	10001	36.76
Alfie Alice Amelia Charlie Daniel Emily Finley Lacey Leah Lexy Luke Riley Tyler	47.91	10010	10002	37.76
Lewis Samuel Scarlett	48.97	10011	22220	37.82
Ellie	63.53	20020	02001	68.18
Eva Harvey	63.53	00110	00201	68.39
Imogen Mohammed Theo	63.82	01010	11020	68.39
George Phoebe	64.45	01020	20111	68.39
Joseph Sophie	64.97	01011	01101	68.86
Charlotte Chloe Leo	65.00	11010	21011	68.86
Olivia	65.10	11100	00200	69.76
Holly Lola Molly	65.16	21000	01102	69.76
Evie	66.69	00120	20110	69.76
Connor	67.42	02000	21012	69.76

Table 2: Pairs and single names from the UK top 50 boys' and girls' names that score highest and lowest playing LOVES. Top section considers pairs of names (complete starting strings); pairs of top-50 names scoring 99%, and number strings arising from top-50 pairs that score $\geqslant 95\%$, are shown. Bottom section considers individual names, and their expected score when playing against all members of the top-50 names lists. The lowest- and highest-scoring ten sets corresponding to top-50 names (left) and from all sets with $c = 3$ (right) are shown.

Discussion

We have explored the behaviour of a popular number game and observed that a simple iterated rule acting on strings of digits produces rich behaviour. Visualising the progress of a game as a trajectory in a space defined by the length of a number string w and the total magnitude of its digits m allows us to identify regions where convergence and divergence is likely, and to characterise the average dynamics underlying movement throughout this space. Based on this picture of the game as a set of steps in (w, m)-space, we have found preliminary results for the probability with which the process corresponding to a given string will terminate, and the dynamics through which this termination or divergence comes about.

Using the most common childrens' names in the UK, we have informally ex-

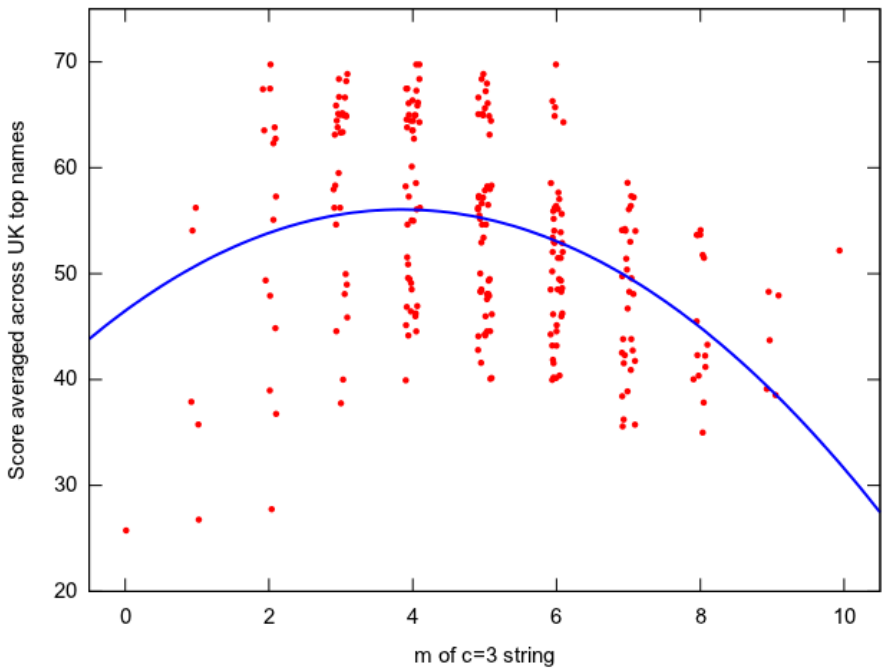

Figure 7: Magnitude of individual $w = 5$, $c = 3$ strings against their averaged score when LOVES is played with all UK top names. For clarity, points are randomly jittered on the x-axis about their (integer) values. Line is a quadratic fit with $r = 0.41$.

plored the ways in which high and convergent scores can be obtained. For both individual names and name pairs, pairs of 'O's are a high-scoring motif; for name pairs, high counts of 'L's can also lead to high scores. For individual names, an intermediate number of LOVES letters confers higher success than cases where all or none are present. Names with no LOVES letters consistently score lowest. The reason for the trend rewarding individual names with intermediate m is unclear, and contrasts with the absence of straightforward predictors of success across complete starting strings (Figure 6). The specific structure of letter counts among UK names (Figs. 3 and 4) likely plays a role in determining this optimum.

Many open questions remain:

1. What features of a terminating string predict the magnitude and value of the final result? What gives rise to the complicated structure describing which final results arise more commonly than others?
2. Equation 4 is rather empirically derived. More rigorously, what are the parameters describing the transition from highly-likely termination to highly-likely divergence as m increases for a given w?
3. What features of a terminating string predict the decay length of the

resulting chain?

4. What are the effects of playing the game in a different base?

5. What patterns result when identical letters in the game word enforce correlations in the initial string (for example, ELSKER, constraining the first and fifth digits to be identical)?

We hope that this informal study of a popular number game has illustrated its rich behaviour to former and new players alike. We suggest that exploring these results, and extending them, may be an engaging pedagogical route for children and students learning about open-ended mathematical investigation and simulation design [2].

Acknowledgements

The author wishes to thank C. Brockington, M. Celuzza, and I. Blaikie for suggesting this investigation, and E. Røyrvik for inspiring it.

References

[1] Bever, K., Rowlett, J. "Love Games: A Game Theory Approach to Compatibility", preprint, arXiv:1312.5483, 2013.

[2] Klawe, M., Phillips, E. "A classroom study: Electronic games engage children as researchers", *The first international conference on Computer support for collaborative learning*, L. Erlbaum Associates Inc., 209–213, 1995.

[3] Papadimitriou, C., Steiglitz, K. *Combinatorial optimization: algorithms and complexity*, Dover, 1998.

[4] Roud, S. *The lore of the playground: One hundred years of children's games, rhymes and traditions*, Random House, 2010.

[5] *Love calculations and paper fortune-tellers* retrieved from `http://www.imisstheoldschool.com/archives/love-calculations-and-chatterbox` at February, 2016.

[6] *UK Office for National Statistics* retrieved from `http://www.ons.gov.uk/ons/rel/vsob1/baby-names--england-and-wales/2010/index.html` at February, 2016.

Appendix

Number of steps to termination, and chain properties

How long must players keep doing sums before they arrive at their final result? To explore this, we define the 'decay length' d as the number of iterations before the game terminates. If a string leads to a looping or divergent outcome, $d = \infty$. Figure 8 shows the distribution of decay lengths for strings in $c = 10$ for various w that terminate. The structure of the game places the restriction that $d \geqslant w - 2$: we cannot terminate in fewer steps because we are limited to a maximum string length decrease of 1 at each step. The decay length distribution is moderately skewed, with some strings taking a considerable time to converge (for example, $\{4, 0, 3, 9, 0\}$ requires 35 iterations to reach $\{2, 2\}$). A noticeable feature of games displaying this slow decay is the presence of $\{1, 0\}$, $\{1, 1\}$ and $\{1, 2\}$ motifs, often in conjunction with 4s, forming medium-magnitude structures which then combine to exceed 9 and replenish the $\{1, [low]\}$ motifs.

What are the dynamics of the chains of strings in these games with long decay lengths? We first explore the maximum string length reached in a chain, as a function of the decay length (Figure 9). Interestingly, very few terminating chains ever contain strings that are much longer than the initial string – suggesting that if the initial string length is exceeded by some amount, divergence is guaranteed. Figure 9 shows that terminating chains from $w = 4$ only very rarely reach length 7; no terminating chains for $w < 7$ reach length 8, and it is very rare for a terminating $w = 7$ chain to reach length 8 (and terminating $w = 7$ chains are themselves rare). The expansion of a $w = 7$ string to a length-8 step occurs in the first iteration of the string $\{1, 0, 0, 0, 1, 9, 1\}$ ($\rightarrow \{1, 0, 0, 1, 1, 0, 1, 0\}$, before terminating at $\{2, 5\}$ after 24 iterations), also illustrating the aforementioned appearance of $\{1, [low]\}$ motifs in slow-decaying chains.

We can also attempt to characterise the dynamics of terminating chains by considering the number of steps in a chain that lead to an increase in string length (Figure 9). Here, the trend is similar across different w (once the longer decay lengths at higher w are taken into account): the number of increasing steps always falls substantially below half of the total number of steps, suggesting that if the decay chain exceeds a certain ratio of length-increasing steps, divergence is guaranteed.

Critical m for a given w

Figure 5 allows us to build a heuristic estimate for properties of a trajectory that avoids non-convergence. First note that the vast majority of $w = 3$ strings converge; the only exceptions are the $\{9, 9, x\}$ strings, which loop if $1 \leqslant x \leqslant 9$. We will neglect these strings and assume that $w = 4$ is the lowest w where a substantial number of strings are non-convergent.

We will consider a trajectory where w decreases from some starting value to $w = 2$, without ever increasing. This picture is overly restrictive: we have seen (Figure 9) that trajectories that experience length increases can still converge. However, for this approximation, we will assume that no length-increasing steps

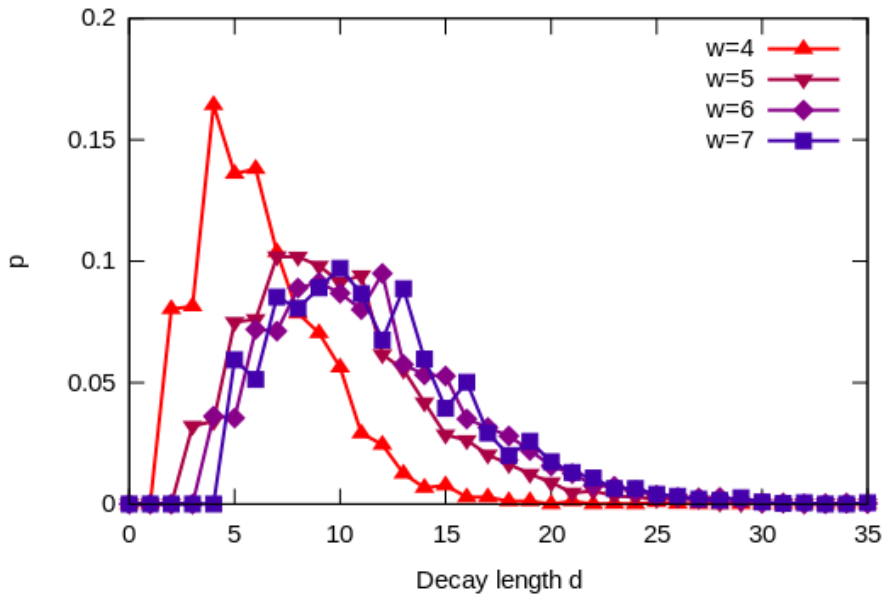

Figure 8: Decay lengths (number of iterations required for a string to terminate) of the $c = 10$ set for different w.

occur ($n = 0$). In this case, the maximum possible value of m after an iteration of the game rule is (from Equation 2):

$$m_{new} = m' - 9n = m' = s_1 + s_w + 2\sum_{i=2}^{w-1} s_i. \tag{6}$$

What are the bounds on m_{new}? If the current string has $m \leqslant 18$, it is straightforward to see that m_{new} is minimised when $s_1 + s_w = m$ and $s_i = 0$ for all other i (concentrating the magnitude in the edge digits, which are not doubled by Equation 6). This situation gives $m_{new} = m$.

The maximum m_{new}, if $w \geqslant 4$ and current $m \leqslant 18$, can be seen to be acheived when the magnitude is concentrated in the sum of Equation 6, and thus doubled. This situation is acheived when $s_1 = s_w = 0$ and $\sum_{i=2}^{w-1} s_i = m$, giving $m_{new} = 2m$. If $w = 3$ and current $m \leqslant 9$, the same reasoning holds. If $w = 3$ and $9 < m \leqslant 18$, m_{new} is maximised by an arrangement where $\sum_{i=2}^{w-1} = 9$ and $s_1 + s_w = m - 9$, giving $m_{new} = m + 9$.

Hence, if $m \leqslant 18$, m_{new} is always bounded from below by m and by above by $2m$ (the $m+9$ bound is enclosed by the $2m$ bound as we have enforced $m > 9$ in this case). Further detailed progress can be made by considering arrangements of digits that induce different values of $n \neq 0$. We will work with the crude approximation that, along a series of non-length-increasing steps, an expected step in m falls in the centre of these bounds. Under this approximation, $m \to \frac{3}{2}m$.

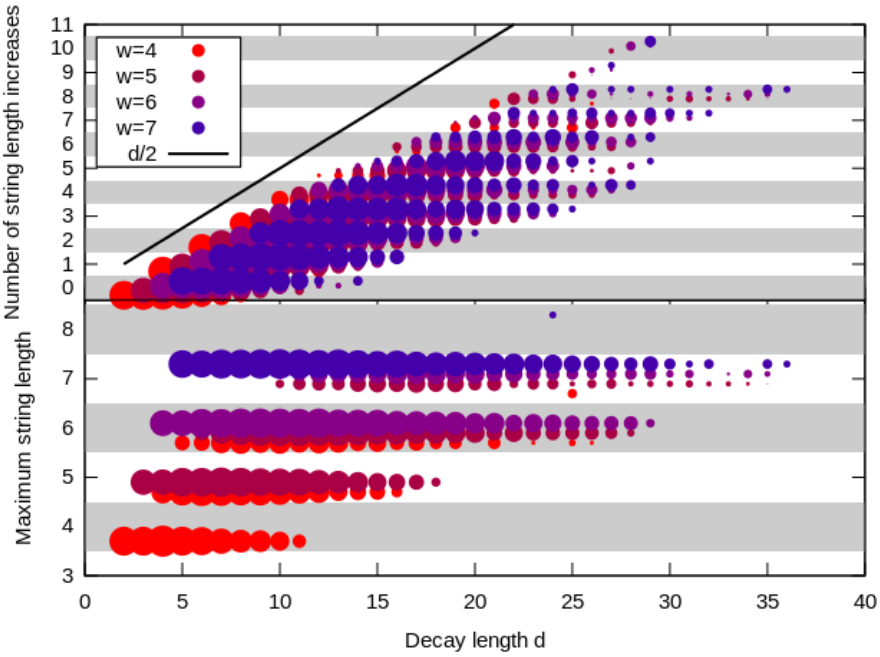

Figure 9: (top) The number of string length increases throughout a game, and (bottom) the maximum string length reached during a game, against the decay length (number of iterations required for a string to terminate) of the $c = 10$ set for different w. Points for different w are offset vertically for clarity.

We have assumed that $w = 4$ is the lowest w with a critical value of m above which non-convergence is likely. Considering the repeated action of approximated steps above from some starting w, we see that to avoid exceeding a given critical value m_c for $w = 4$, we require $m < m_c/(3/2)^{w-4}$.

What value of m_c can be chosen to avoid divergence? Consider the maximum m we can achieve for $w = 4$ with $n = 0$ (no length-increasing steps). This is achieved by strings that, upon iteration, give $\{9, 9, 9\}$ – for example, $\{4, 5, 4, 5\}$ (among others). The maximum m for which $n = 0$ at $w = 4$ is thus readily seen to be 18, and we set $m_c = 18$ to follow this line of reasoning. We see in Figure 5 that $m^* = 18/(3/2)^{w-4}$ gives a reasonable theoretical prediction of the position of the transitional m for a given w.

As something of an aside, we can also place bounds on the minimum magnitude required to support a given value of n. It will be observed that the lowest-magnitude strings of adjacent pairs that give rise to n sums $\geqslant 10$ are $\{1, 9\}$ (among others for $n = 1$); $\{1, 9, 1\}$ ($n = 2$); $\{1, 9, 1, 9\}$ ($n = 3$); $\{1, 9, 1, 9, 1\}$ ($n = 4$); etc. The minimum m required to support a given n is thus:

$$m_{min}(n) = 10\frac{n+1}{2} + (1 - n \bmod 2) \tag{7}$$

Backtracking

Simple algebra shows that, if no steps occur that increase string length, the digits in a decay chain starting from $w = 5$ and ending at $w = 2$ are given by the expressions in Table 3.

A similar set of expressions could be derived in a large number of ways, by choosing the unknown values a_1, a_2, a_3 to lie not at the start of each string but at other positions within each. Clearly, to give a valid decay chain with no length-expanding transitions, all the elements in Table 3 must lie between 0 and 9. The resulting set of inequalities restricting choices of a_1, a_2, and a_3 is complicated and, while straightforwardly addressable numerically with integer programming, has prevented further intuitive progress.

s_1	s_2			
a_1	$s_1 - a_1$	$s_2 - s_1 + a_1$		
a_2	$a_1 - a_2$	$s_1 - 2a_1 + a_2$	$s_2 - 2s_1 + 3a_1 - a_2$	
a_3	$a_2 - a_3$	$a_1 - 2a_2 + a_3$	$s_1 - 3a_1 + 3a_2 - a_3$	$s_2 - 3s_1 + 6a_1 - 4a_2 + a_3$

Table 3: Backtracked values of a $w = 5$ string giving a final result $\{s_1, s_2\}$ with the assumption of no length-increasing steps. Table rows run backwards through iterations of the game rules; at each backwards step, a new variable a_i is introduced. All elements in this table must lie between 0 and 9 inclusive for this decay chain to be valid.